Precision Calculation of the *x*-dependence of PDFs from Lattice QCD

Fermilab Theory Seminar

YONG ZHAO

MAY 06, 2021

Argonne NATIONAL LABORATORY

High-energy proton structure and the parton model

- The inner proton structure has been probed via processes such as deep inelastic (e.g., e^-+p) scatterings.

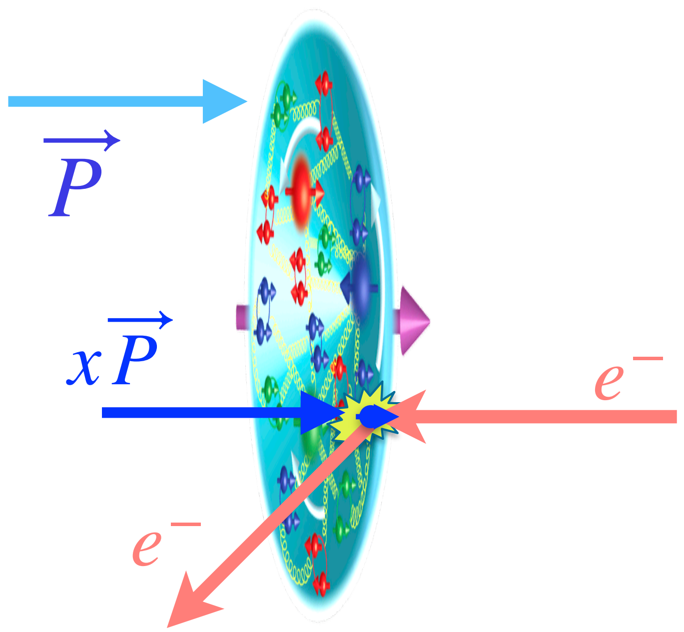

Richard P. Feynman

Feynman's parton model (1969):

- Quarks and gluons are "frozen" in the transverse plane due to Lorentz contraction;
- During a hard collision, the struck quark/gluon (parton) appears to the probe that it does not interact with its surroundings.

Parton distribution functions (PDFs)

- Unpolarized PDF $f_i(x)$:

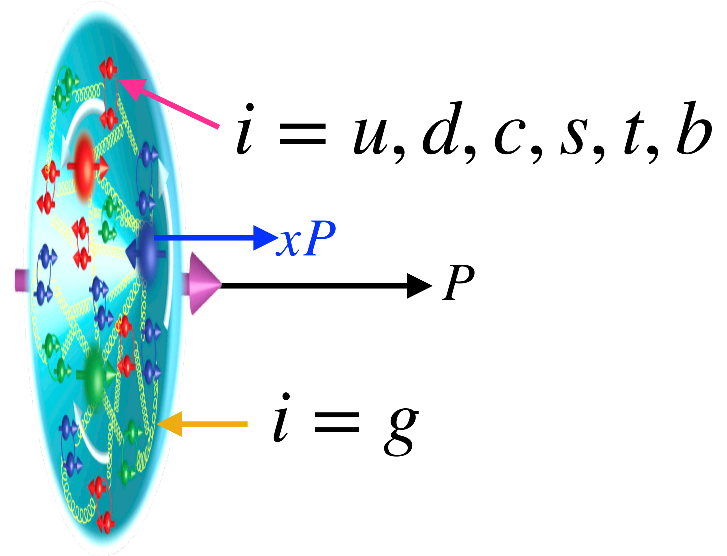

- Helicity PDF $\Delta f_i(x)$:

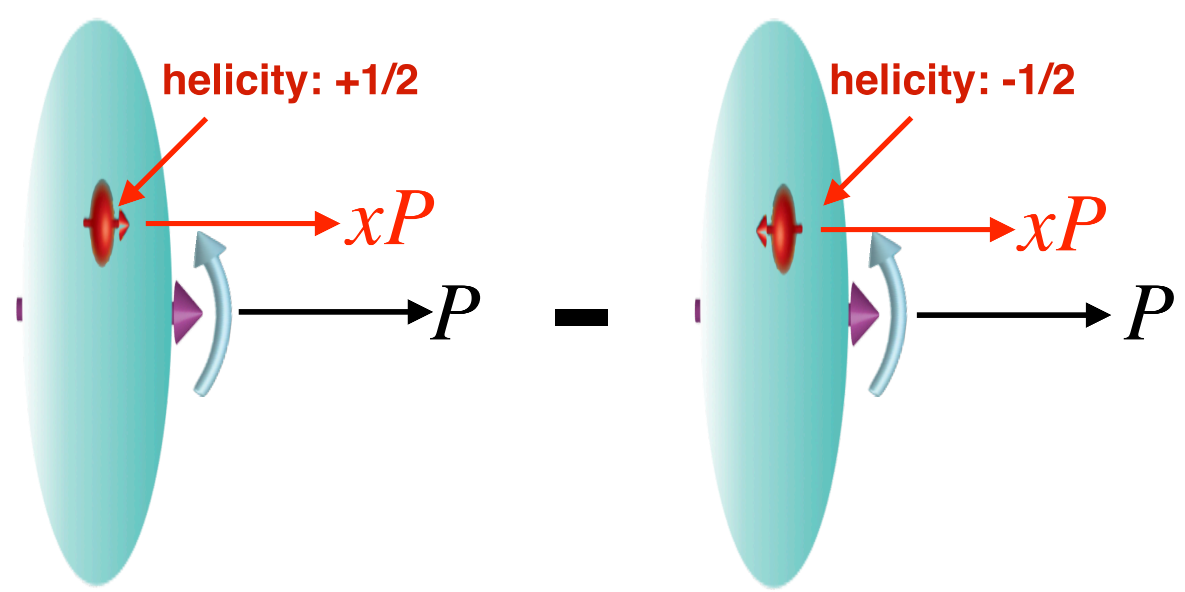

PDFs and precision tests for the Standard Model

- PDFs are the basic inputs for Standard Model predictions in high-energy scattering experiments.

Nonperturbative and not well known 🙁

Higgs production from gluon-gluon fusion at LHC:

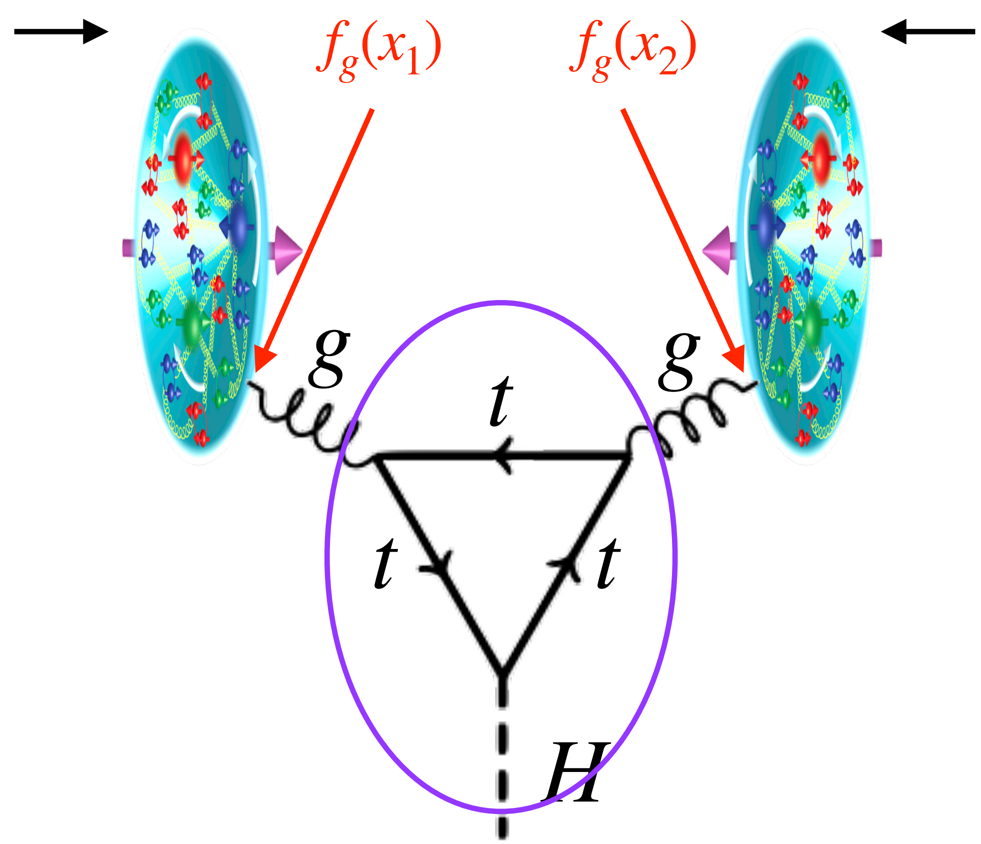

$$\sigma = f_g(x_1)\, f_g(x_2)\, \hat{\sigma}_{gg\to H}$$

Perturbative and well known 🙂

PDFs and precision tests for the Standard Model

- PDFs are the basic inputs for Standard Model predictions in high-energy scattering experiments.

Nonperturbative and not well known 🙁

Higgs production from gluon-gluon fusion at LHC:

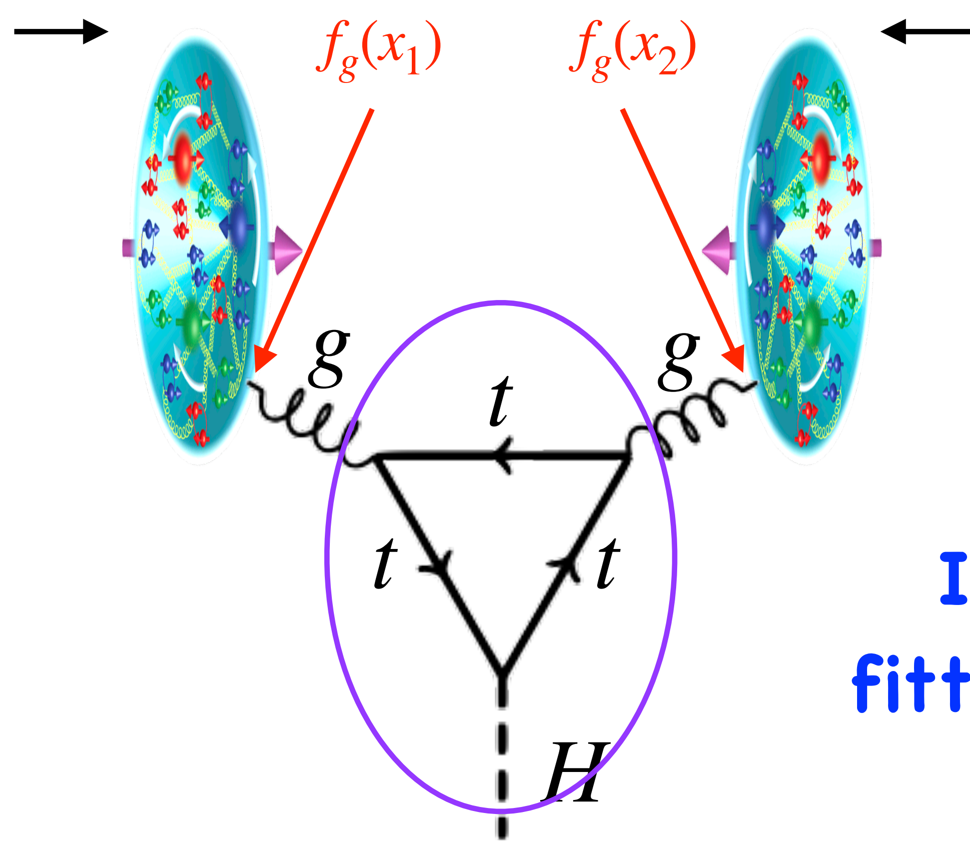

$$\sigma = f_g(x_1)\, f_g(x_2)\, \hat{\sigma}_{gg\to H}$$

In reverse, PDFs can be fitted from a global analysis of experimental data!

Perturbative and well known 🙂

PDFs from experiments

- The PDFs have been measured extensively at the state-of-the-art accelerator experiments since the late 1960s.

SLAC, US

DESY, Germany

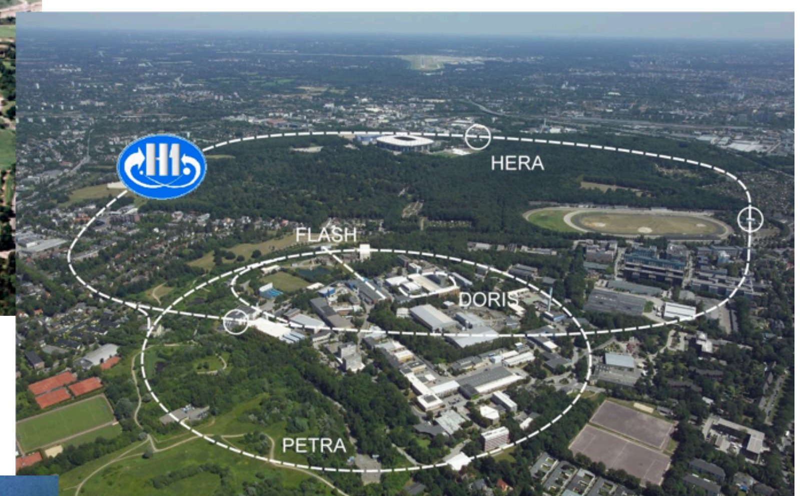

FermiLab, US

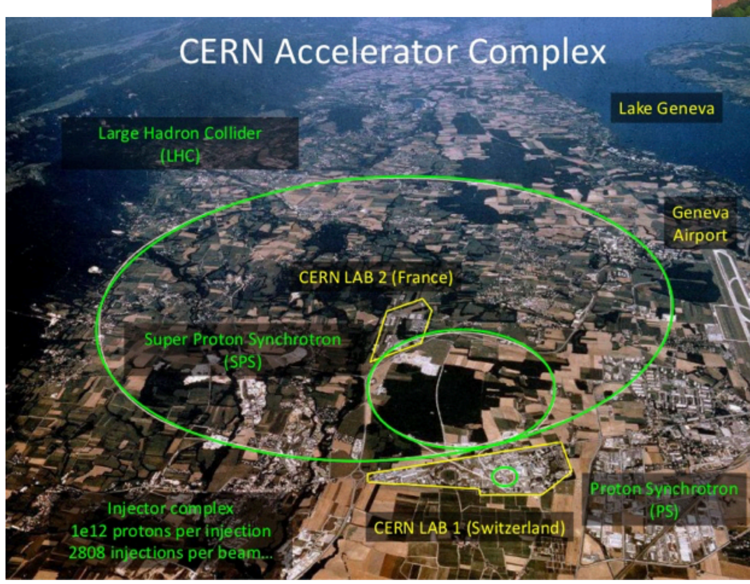

CERN, Europe

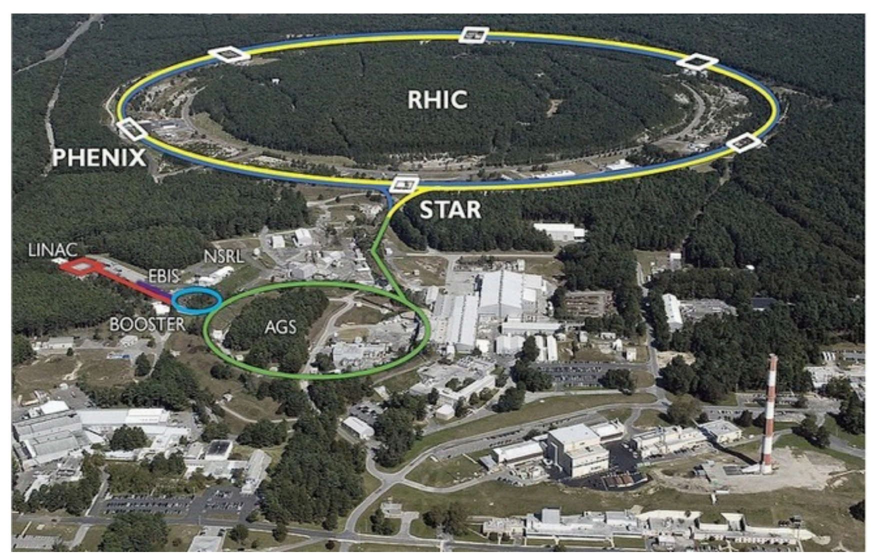

RHIC@BNL, US

Jefferson Lab, US

PDFs from experiments

- The next-generation machine: the Electron-Ion Collider (EIC)

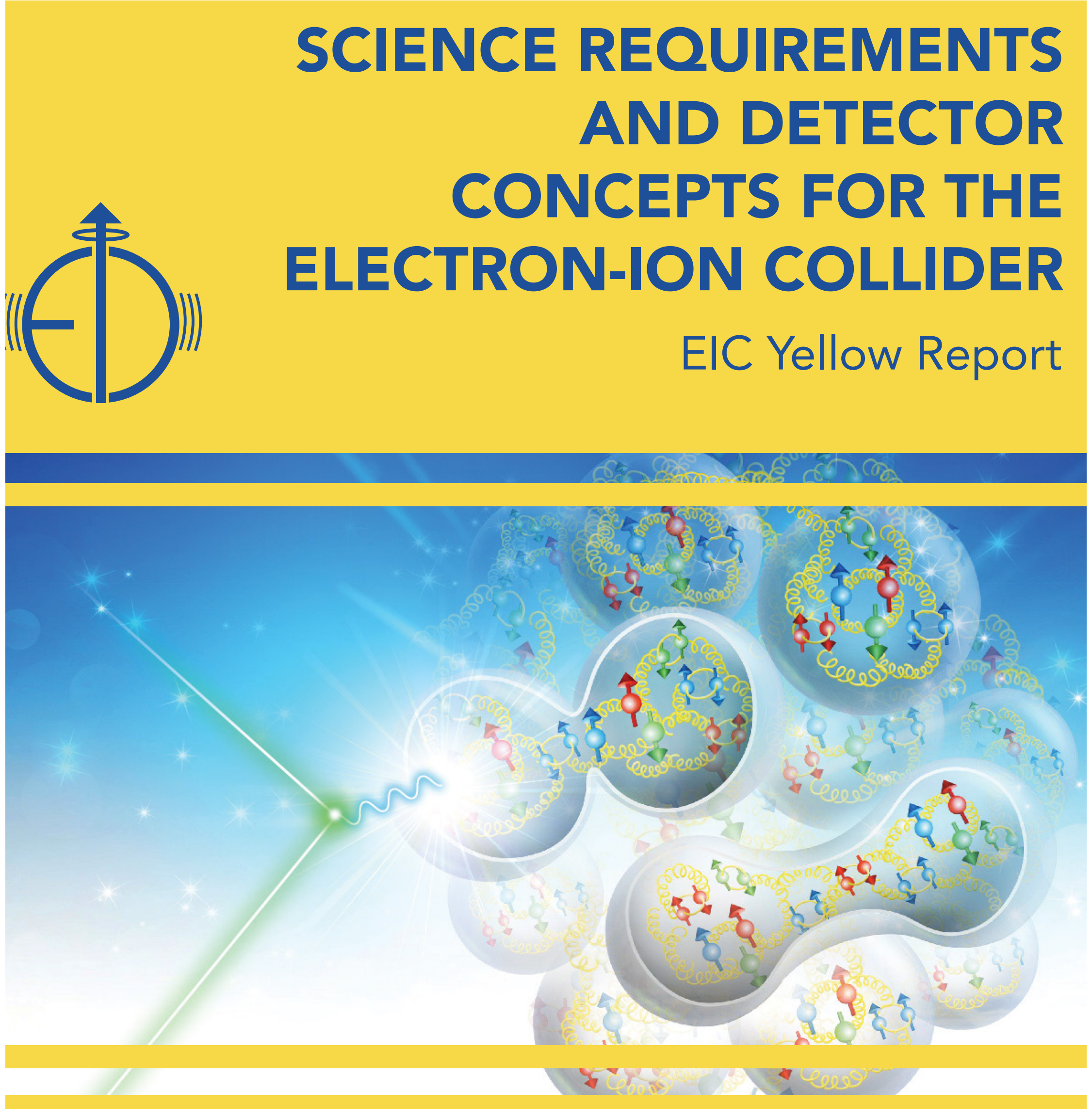

EIC Yellow Report,

R. Abul Khalek et al., 2103.05419.

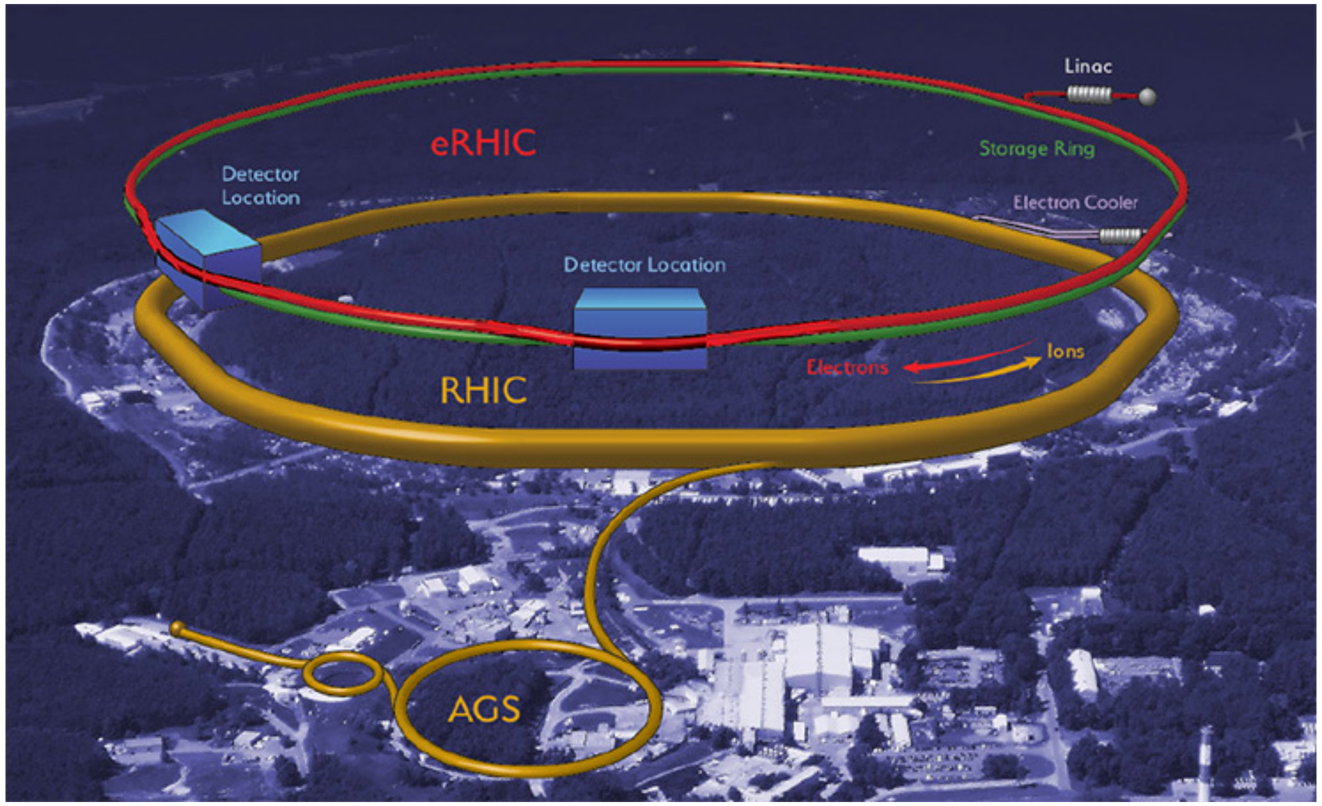

$1.6—2.6 Billion, to be completed in 2030.

An approximate picture of the PDF

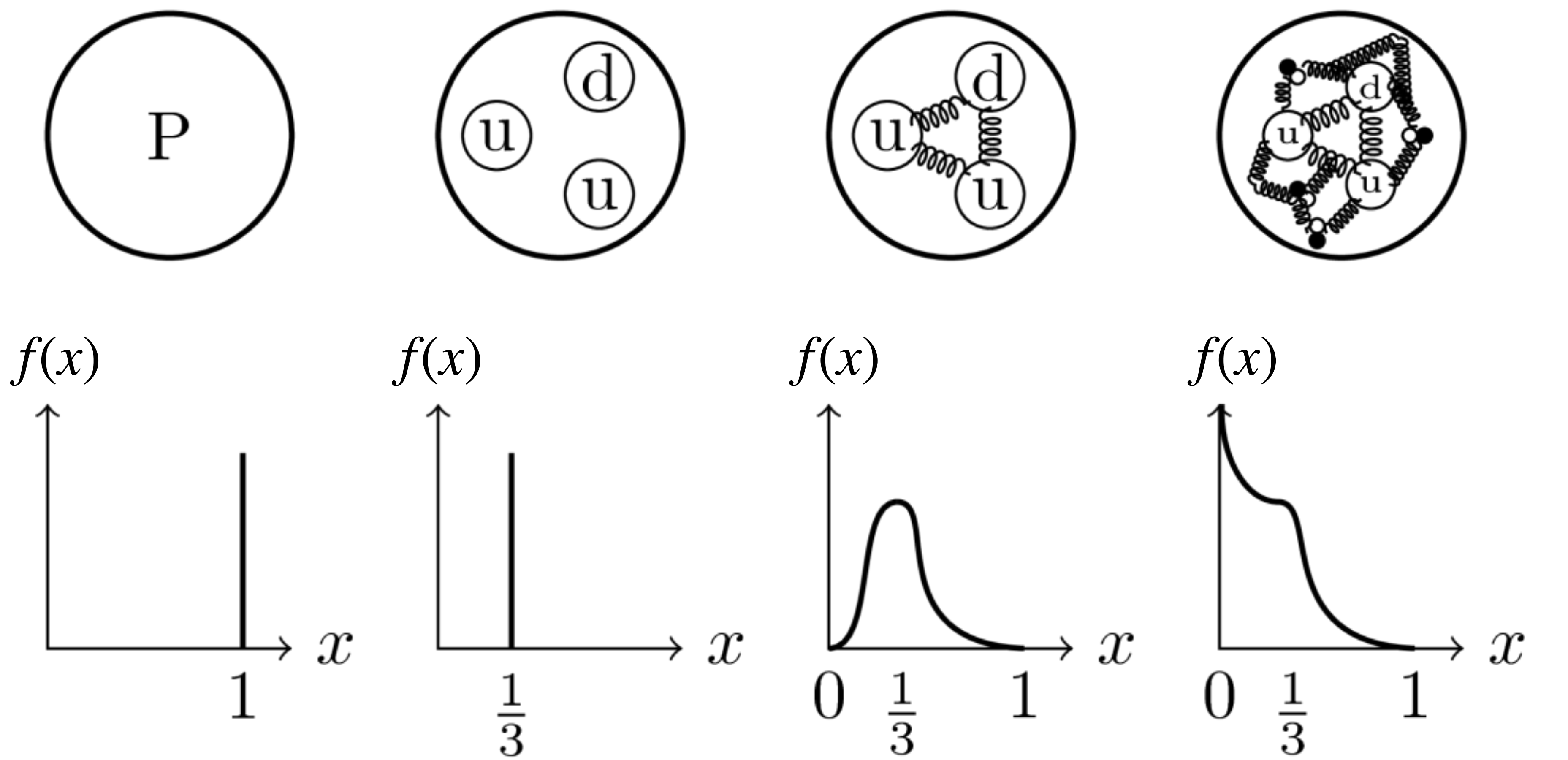

Picture credit,
Fernanda Steffans

No proton substructure | 3 free valence quarks | 3 bound valence quarks | 3 valence quarks + sea + gluons

An approximate picture of the PDF

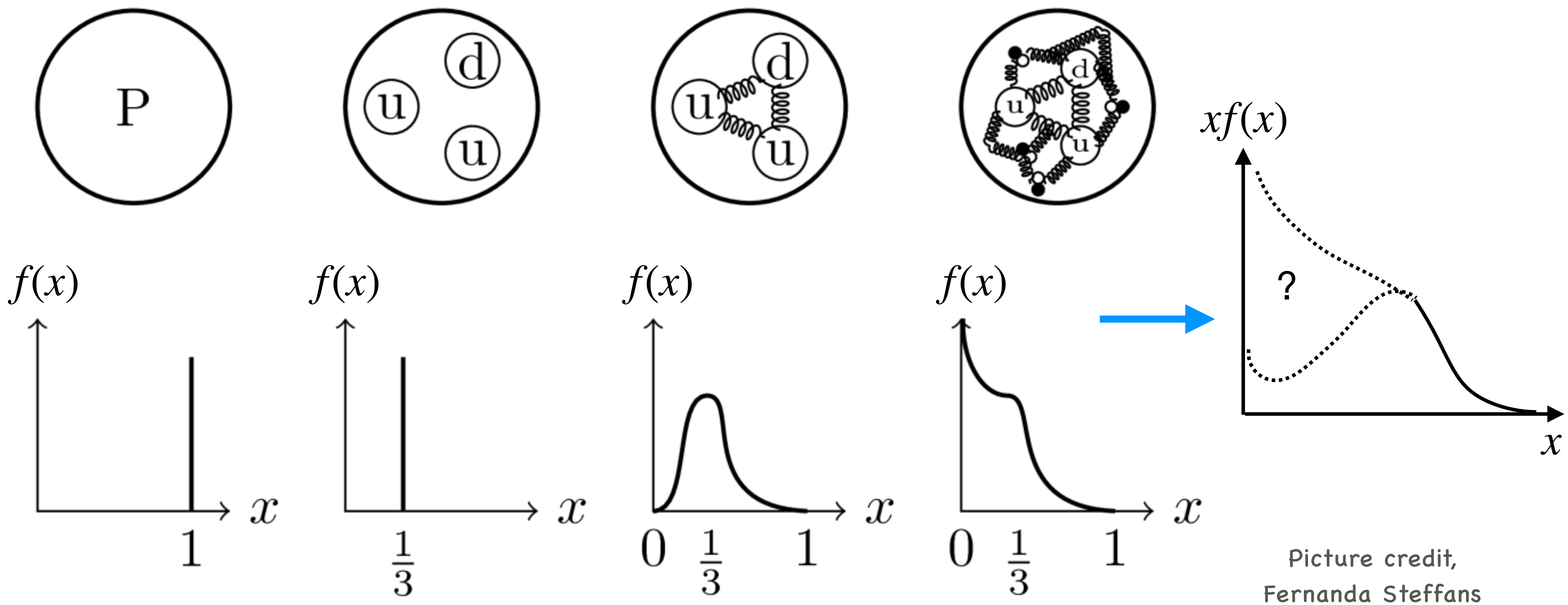

Picture credit,
Fernanda Steffans

No proton substructure

3 free valence quarks

3 bound valence quarks

3 valence quarks + sea + gluons

PDFs from experiments

Unpolarized PDF

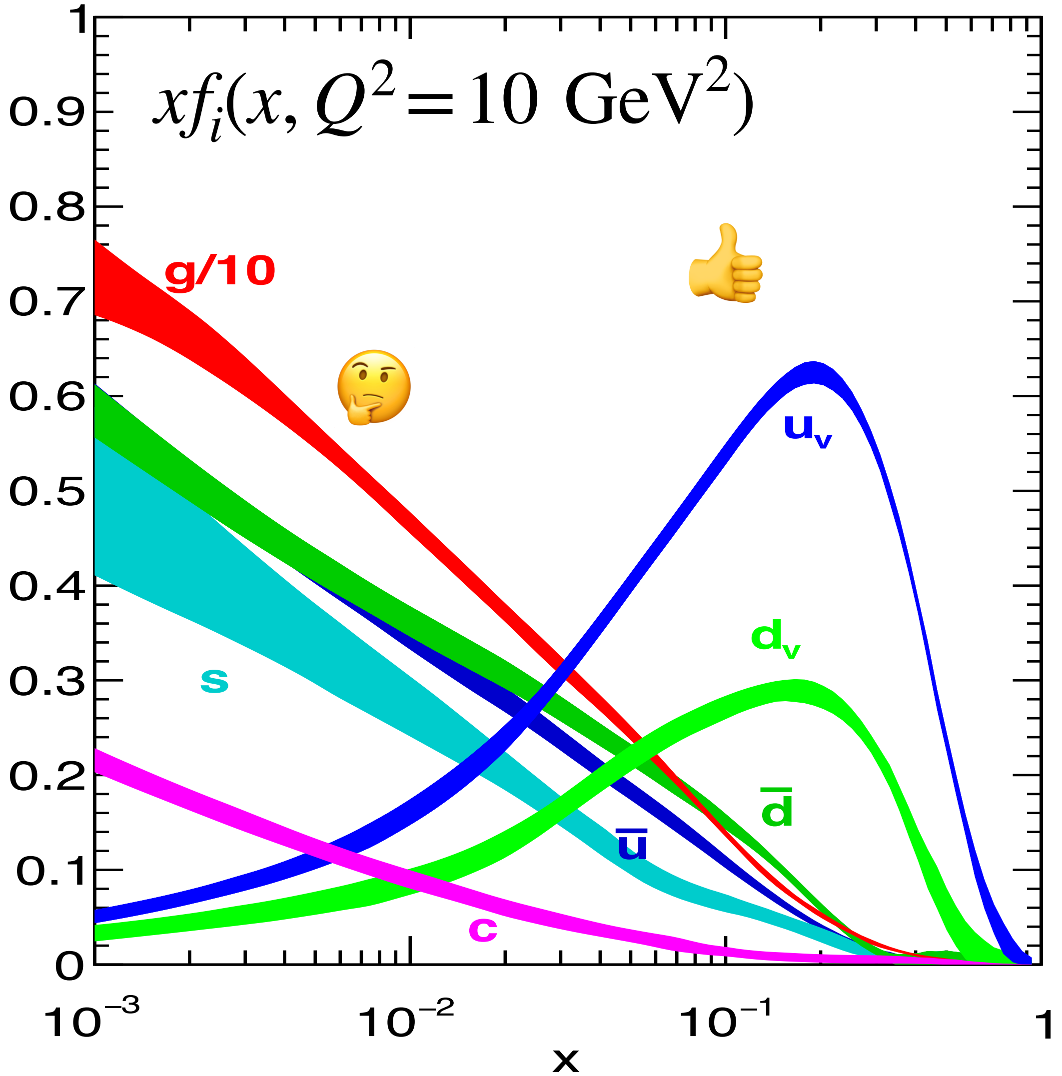

NNPDF Collaboration, EPJ C77 (2017)

PDFs from experiments

Unpolarized PDF

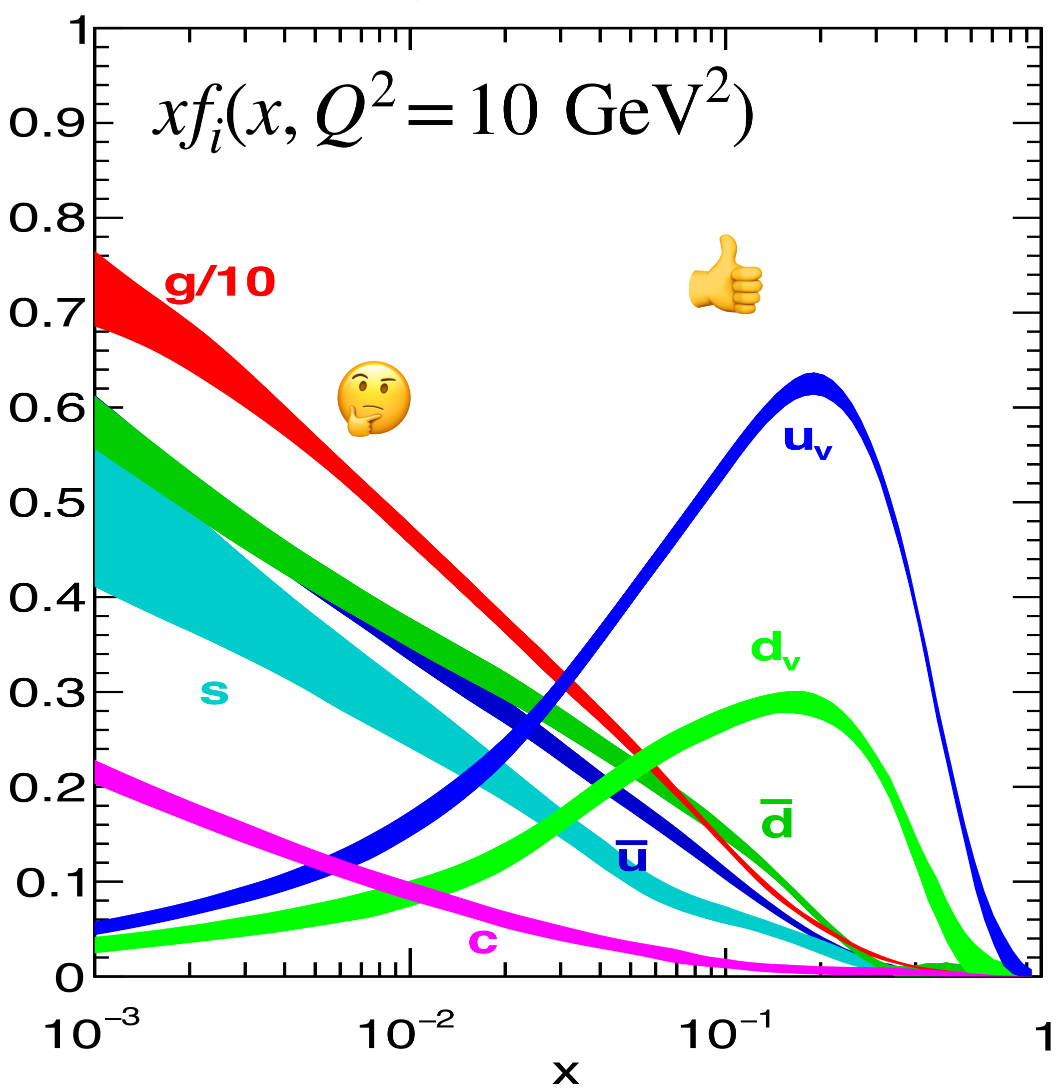

NNPDF Collaboration, EPJ C77 (2017)

Helicity PDF

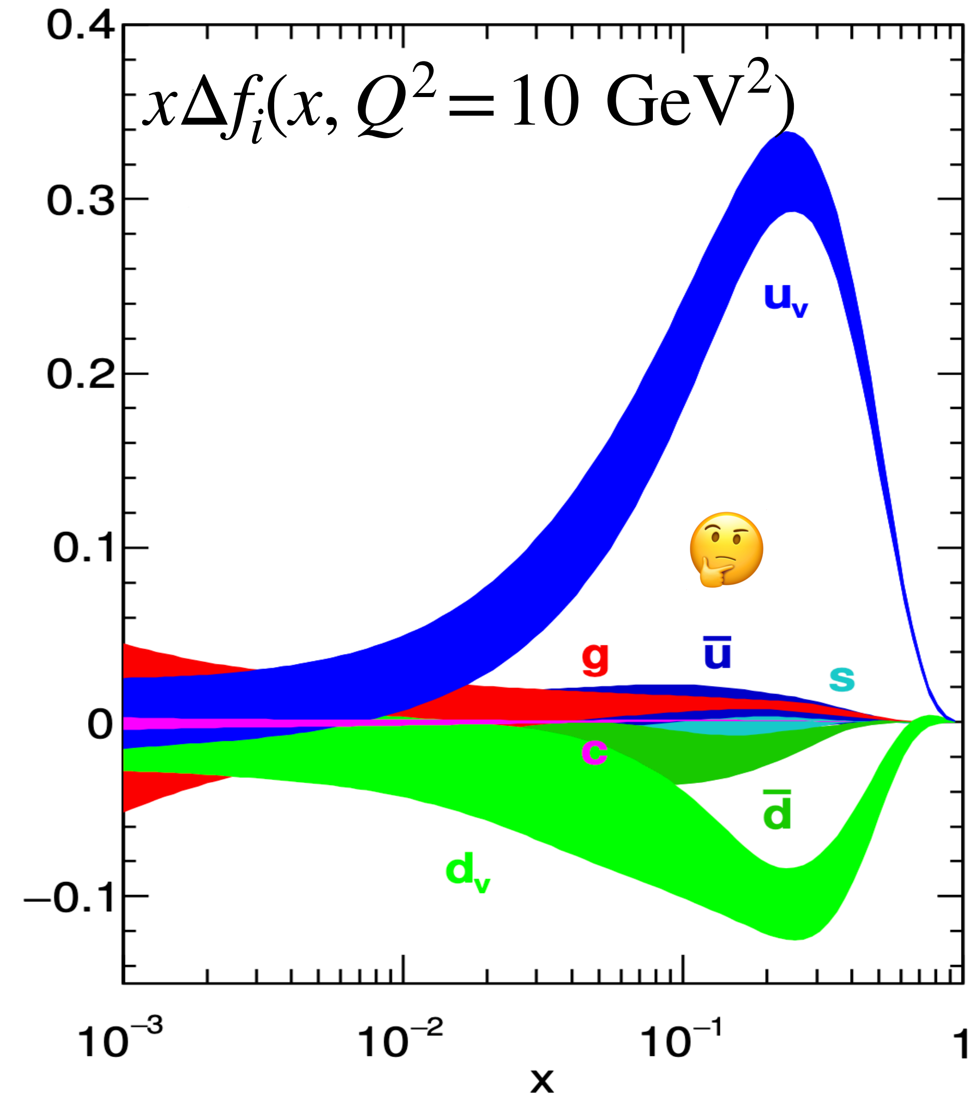

NNPDFpol1.1, Particle Data Group (2019)

PDFs from experiments

Ratios of sea quark distributions, $\bar{d}(x)/\bar{u}(x)$

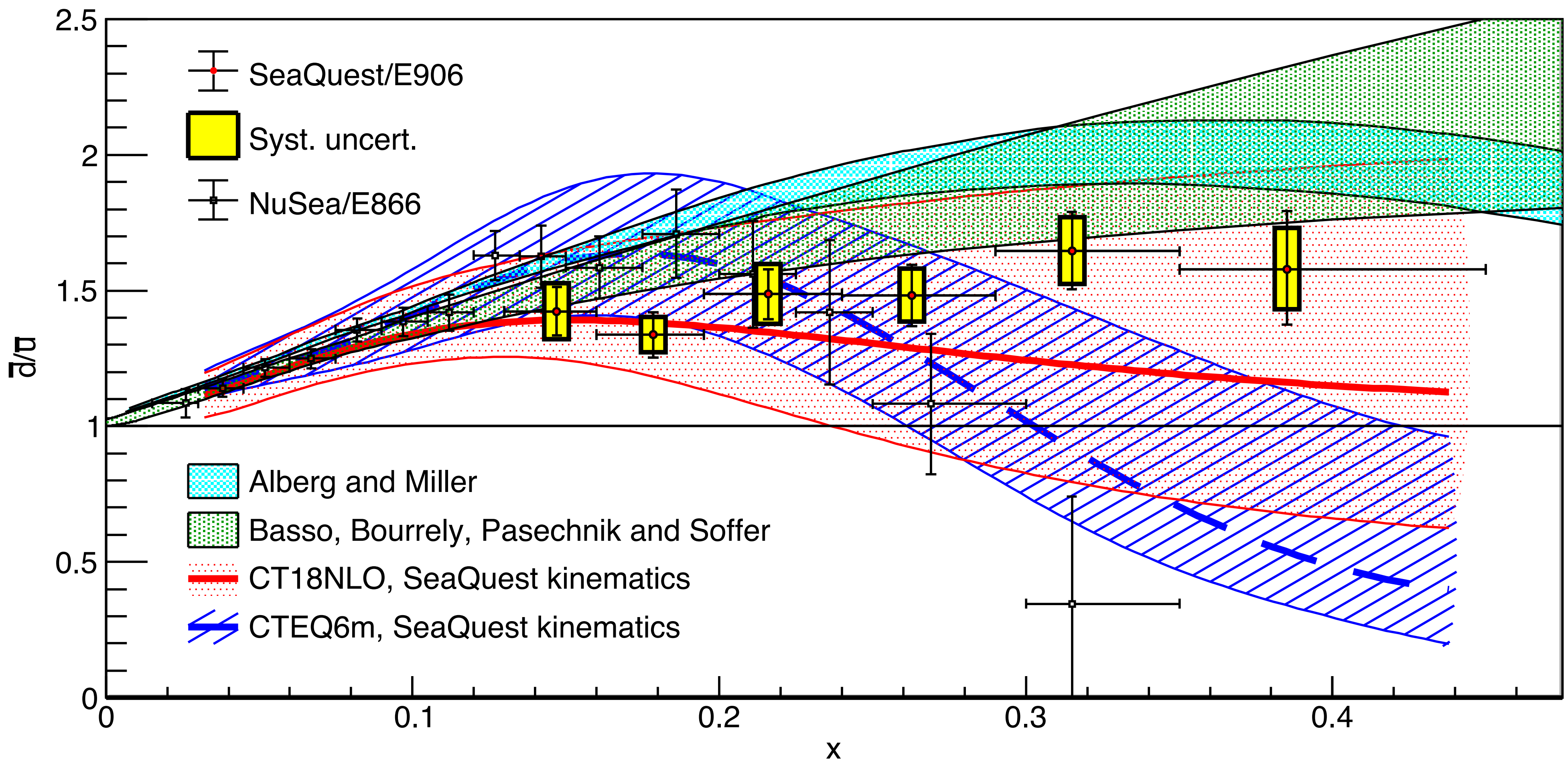

SeaQuest Collaboration, Nature 590 (2021).

PDFs from experiments

World data on the spin-dependent structure function $g_1(x, Q^2)$

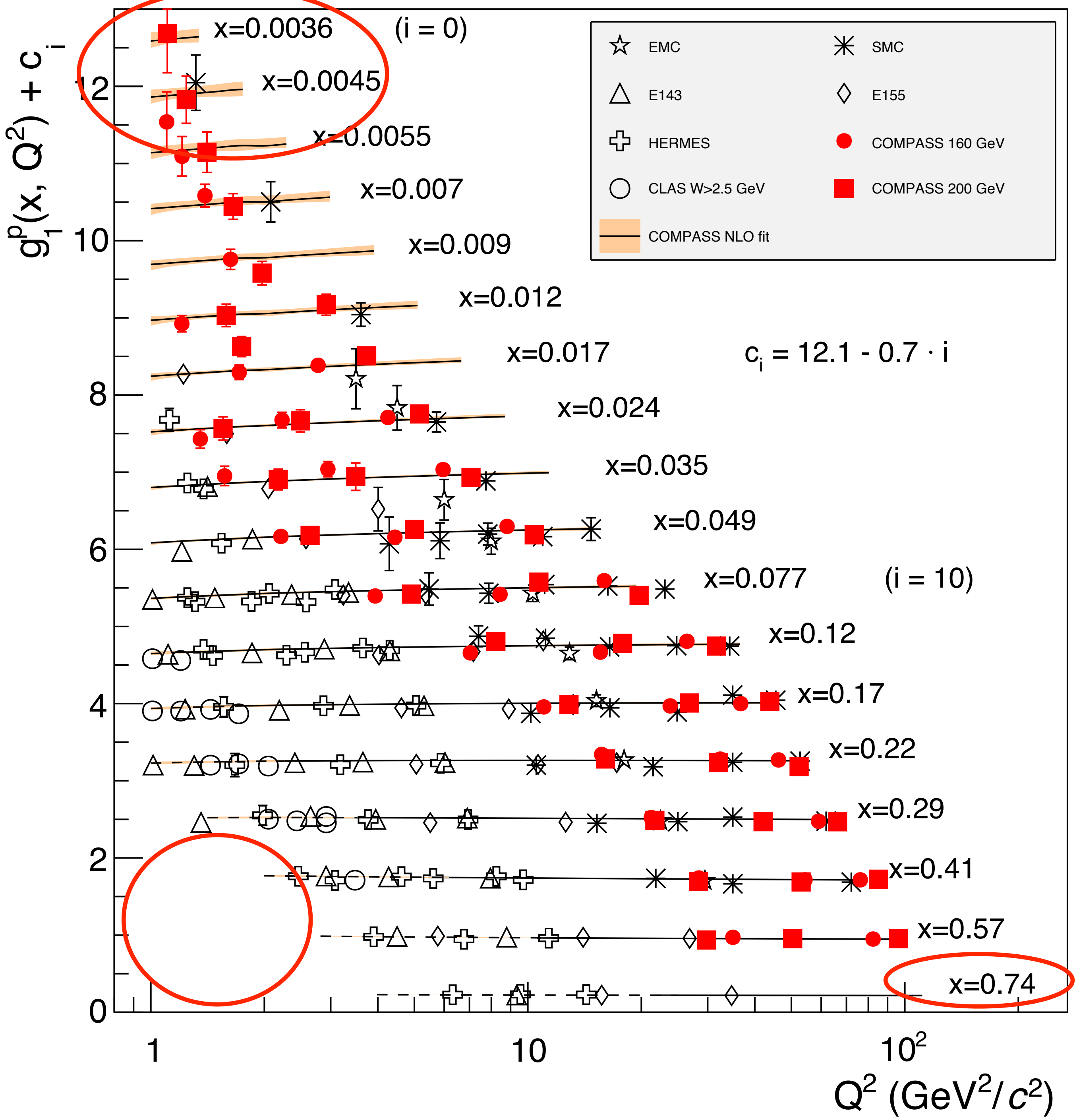

First-principles calculation of (spin-dependent) PDFs can provide important complementary information to the global analysis!

Particle Data Group, 2019

Lattice QCD

- Lattice gauge theory (1974): a systematically improvable approach to solve non-perturbative QCD.

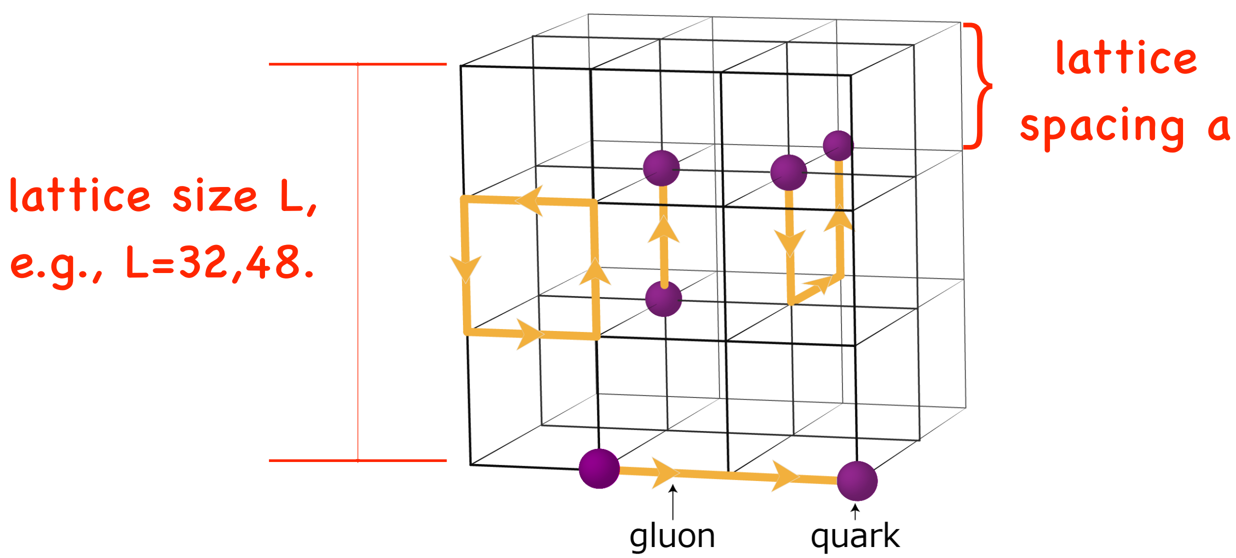

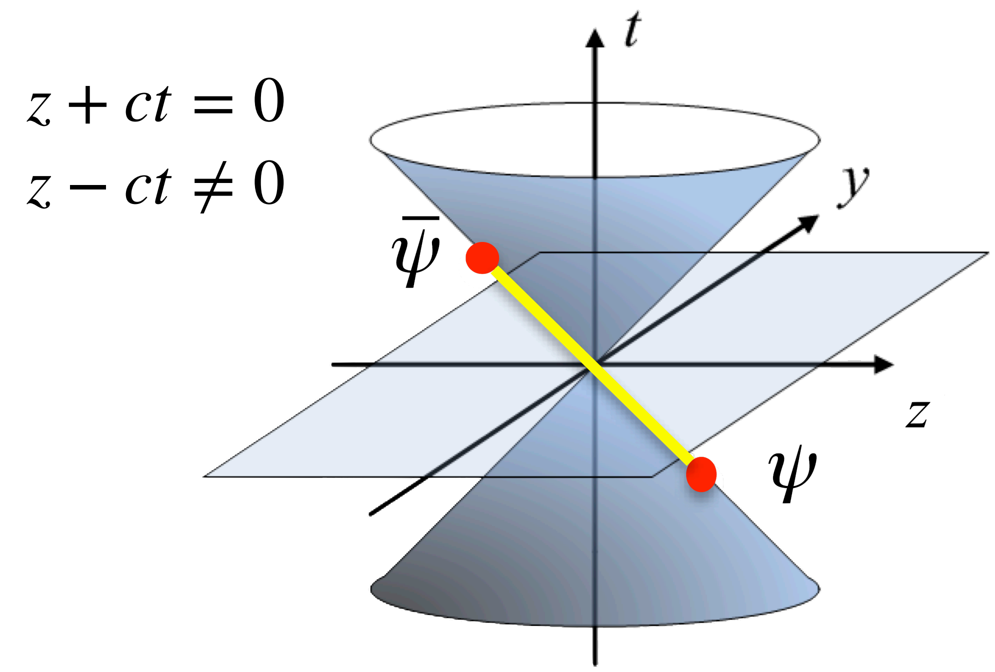

Imaginary time: $t \to i\tau$ $\quad O(i\tau) \overset{?}{\to} O(t)$

Partonic observables are defined on the light-cone

Simulating real-time dynamics has been extremely difficult due to the issue of analytical continuation. 🙁

Large-Momentum Effective Theory (LaMET)

$z + ct = 0, \;\; z - ct \neq 0$

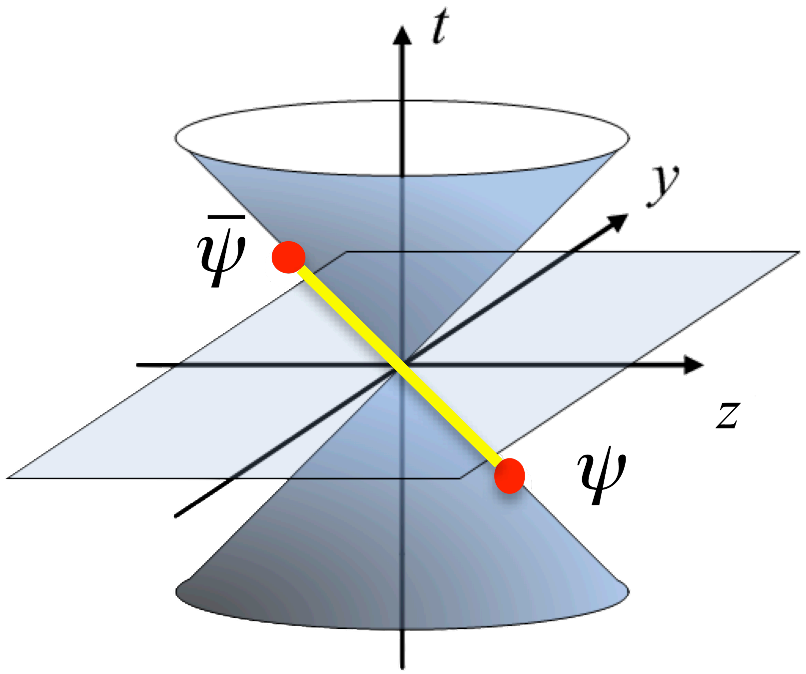

PDF $f(x)$:
Cannot be calculated
on the lattice

$$f(x) = \int \frac{db^-}{2\pi} e^{-ib^-(xP^+)} \langle P | \bar{\psi}(b^-) \times \frac{\gamma^+}{2} W[b^-, 0] \psi(0) | P \rangle$$

$t = 0, \;\; z \neq 0$

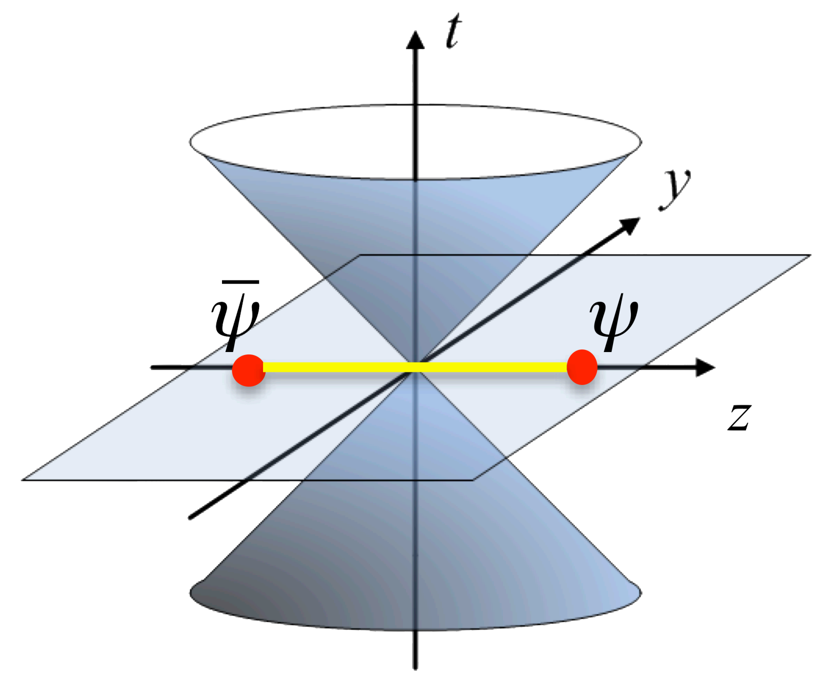

Quasi-PDF $\tilde{f}(x, P^z)$:
Directly calculable on
the lattice

$$\tilde{f}(x, P^z) = \int \frac{dz}{2\pi} e^{ib^z(xP^z)} \langle P | \bar{\psi}(b^z) \times \frac{\gamma^z}{2} W[b^z, 0] \psi(0) | P \rangle$$

Large-Momentum Effective Theory (LaMET)

$z + ct = 0, \quad z - ct \neq 0$

Related by Lorentz boost

$t = 0, \quad z \neq 0$

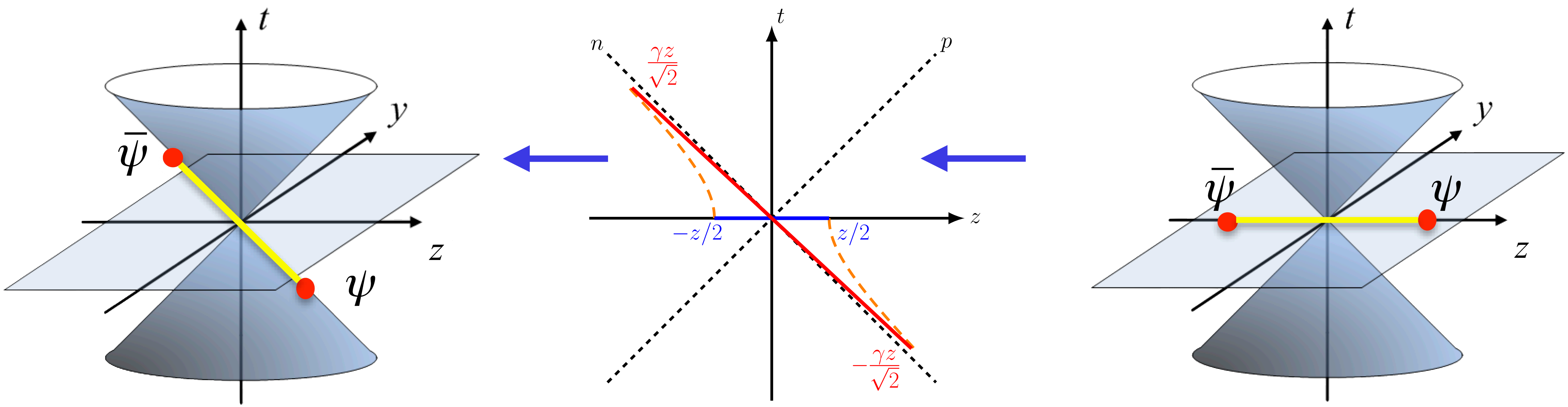

PDF $f(x)$:
Cannot be calculated on the lattice

$$f(x) = \int \frac{db^-}{2\pi} e^{-ib^-(xP^+)} \langle P | \bar{\psi}(b^-) \times \frac{\gamma^+}{2} W[b^-,0] \psi(0) | P \rangle$$

Quasi-PDF $\tilde{f}(x, P^z)$:
Directly calculable on the lattice

$$\tilde{f}(x, P^z) = \int \frac{dz}{2\pi} e^{ib^z(xP^z)} \langle P | \bar{\psi}(b^z) \times \frac{\gamma^z}{2} W[b^z,0] \psi(0) | P \rangle$$

Large-Momentum Effective Theory (LaMET)

$z + ct = 0, \;\; z - ct \neq 0$

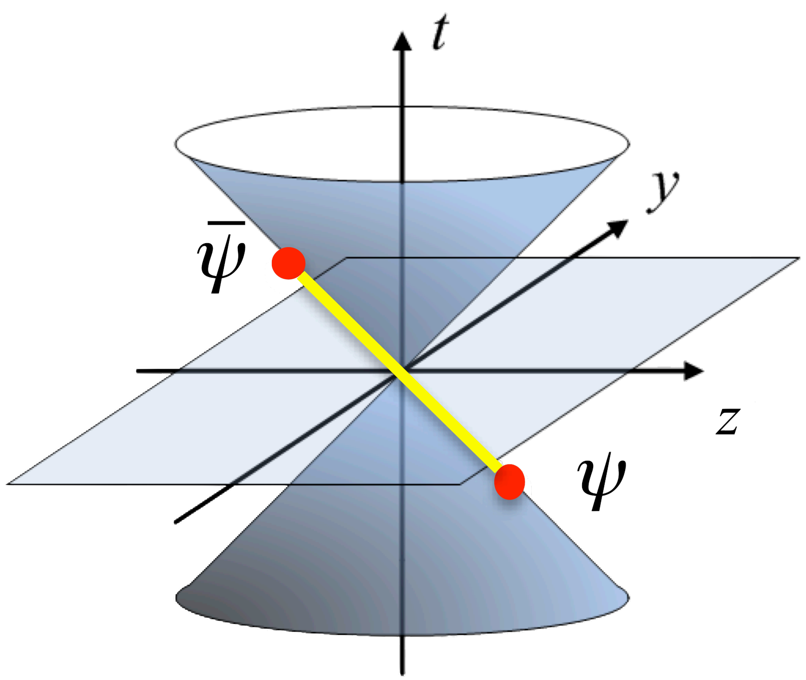

Related by Lorentz boost

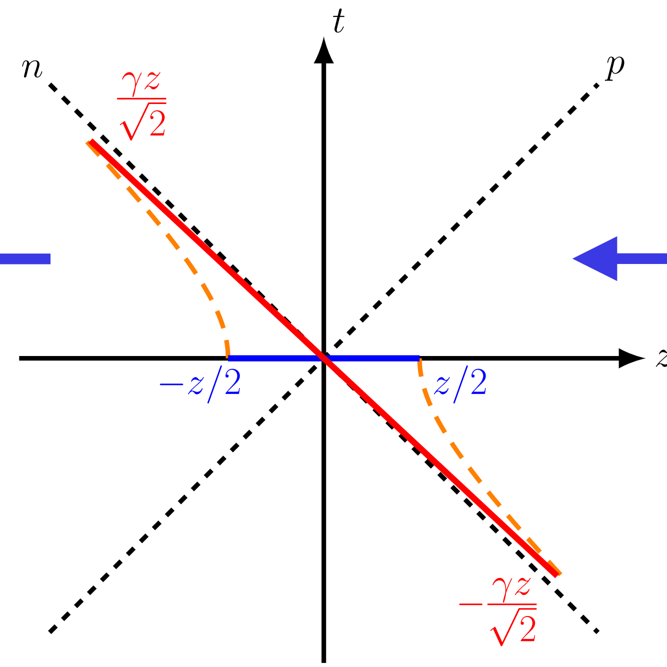

$t = 0, \;\; z \neq 0$

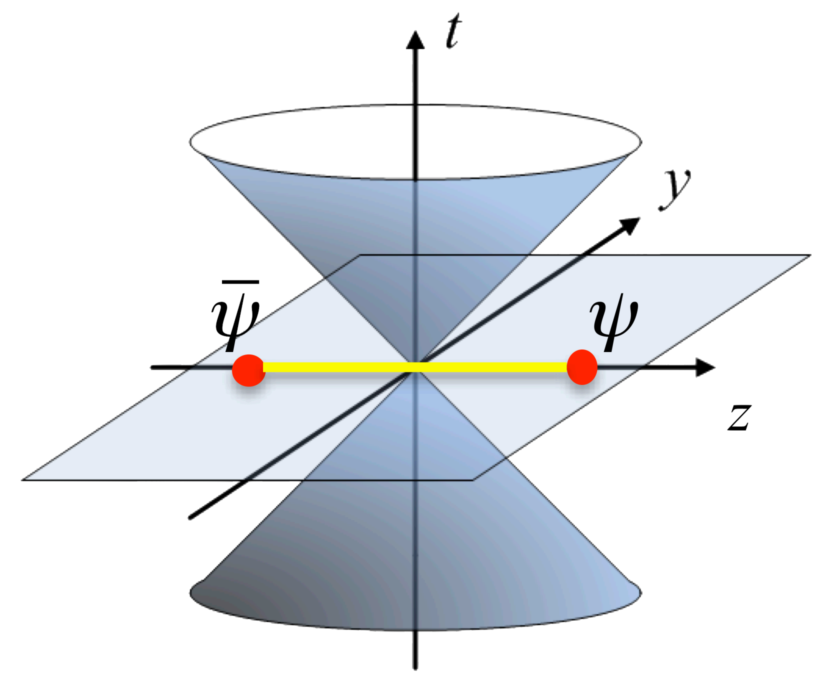

PDF $f(x)$:
Cannot be calculated on the lattice

$$f(x) = \int \frac{db^-}{2\pi} e^{-ib^-(xP^+)} \langle P | \bar{\psi}(b^-) \times \frac{\gamma^+}{2} W[b^-,0] \psi(0) | P \rangle$$

$$\lim_{P^z \to \infty} \tilde{f}(x, P^z) \overset{?}{=} f(x)$$

Quasi-PDF $\tilde{f}(x, P^z)$:
Directly calculable on the lattice

$$\tilde{f}(x, P^z) = \int \frac{dz}{2\pi} e^{ib^z(xP^z)} \langle P | \bar{\psi}(b^z) \times \frac{\gamma^z}{2} W[b^z,0] \psi(0) | P \rangle$$

Large-Momentum Effective Theory (LaMET)

$z + ct = 0, \;\; z - ct \neq 0$

Related by Lorentz boost

$t = 0, \;\; z \neq 0$

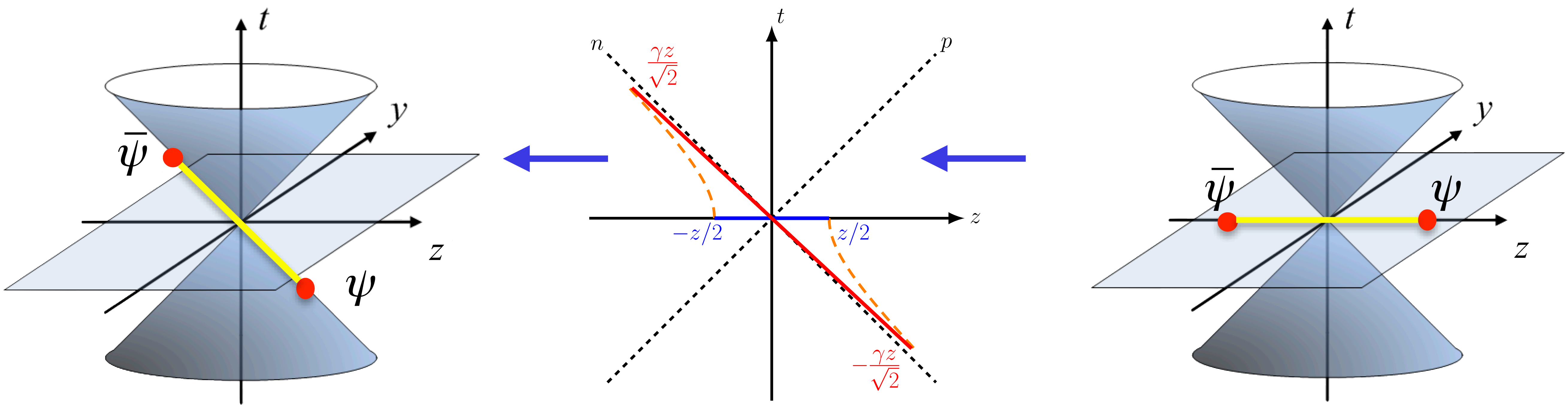

PDF $f(x)$:
Cannot be calculated on the lattice

$$f(x) = \int \frac{db^-}{2\pi} e^{-ib^-(xP^+)} \langle P | \bar{\psi}(b^-) \times \frac{\gamma^+}{2} W[b^-,0] \psi(0) | P \rangle$$

$$\lim_{P^z \to \infty} \tilde{f}(x, P^z) \stackrel{?}{=} f(x)$$

Quasi-PDF $\tilde{f}(x, P^z)$:
Directly calculable on the lattice

$$\tilde{f}(x, P^z) = \int \frac{dz}{2\pi} e^{ib^z(xP^z)} \langle P | \bar{\psi}(b^z) \times \frac{\gamma^z}{2} W[b^z,0] \psi(0) | P \rangle$$

Large-Momentum Effective Theory (LaMET)

- Quasi-PDF: $P^z \ll \Lambda$;

Λ: the ultraviolet lattice cutoff, $\sim 1/a$

- PDF: $P^z = \infty$, including $P^z \gg \Lambda$.
  - The limits $P^z \ll \Lambda$ and $P^z \gg \Lambda$ are not exchangeable;
  - For $P^z \gg \Lambda_{\rm QCD}$, their infrared (nonperturbative) physics are the same.

$$\tilde{f}(x, P^z) = \boxed{C\left(x, P^z/\mu\right)} \otimes f(x, \mu) + O\Big(\frac{\Lambda_{\rm QCD}^2}{P_z^2}\Big)$$

Perturbative matching

Power corrections

- It is the large-momentum state, instead of the operator, that filters out collinear modes in the field operators;
- Contribution from the collinear modes is identical to the PDF.

- X. Ji, PRL 110 (2013); SCPMA57 (2014).
- X. Xiong, X. Ji, J.-H. Zhang and YZ, PRD 90 (2014);
- X. Ji, Y.-S. Liu, Y. Liu, J.-H. Zhang and YZ, arXiv: 2004.03543.

Large-Momentum Effective Theory (LaMET)

- Factorization formula:

$$\tilde{f}(y, P^z) = \int_{-1}^{1} \frac{dx}{|x|} C\left(\frac{y}{x}, \frac{\mu}{xP^z}\right) f(x, \mu) + \mathcal{O}\left(\frac{\Lambda_{\rm QCD}^2}{(yP^z)^2}, \frac{\Lambda_{\rm QCD}^2}{((1-y)P^z)^2}\right)$$

- X. Ji, PRL 110 (2013); SCPMA57 (2014);
- X. Xiong, X. Ji, J.-H. Zhang and YZ, PRD 90 (2014);
- Y.-Q. Ma and J. Qiu, PRD98 (2018), PRL 120 (2018);
- T. Izubuchi, X. Ji, L. Jin, I. Stewart, and YZ, PRD98 (2018).
- X. Ji, Y.-S. Liu, Y. Liu, J.-H. Zhang and YZ, arXiv: 2004.03543.

- The formula can be inverted order by order in α_s:

$$f(x, \mu) = \int_{-\infty}^{\infty} \frac{dy}{|y|} C^{-1}\left(\frac{x}{y}, \frac{\mu}{yP^z}\right) \tilde{f}(y, P^z) + \mathcal{O}\left(\frac{\Lambda_{\rm QCD}^2}{(xP^z)^2}, \frac{\Lambda_{\rm QCD}^2}{((1-x)P^z)^2}\right)$$

Controlled power expansion for $x \in [x_{\rm min}, x_{\rm max}]$ at finite P^z

Precision calculation of the x-dependence of PDFs

- Large-momentum expansion:

$$f(x,\mu) = \int_{-\infty}^{\infty} \frac{dy}{|y|} C\left(\frac{x}{y}, \frac{\mu}{yP^z}\right) \tilde{f}(y, P^z, \mu) + \mathcal{O}\left(\frac{\Lambda^2_{\rm QCD}}{(xP^z)^2}, \frac{\Lambda^2_{\rm QCD}}{((1-x)P^z)^2}\right)$$

State-of-the-art: next-to-next-to-leading order (NNLO) matching for the non-singlet quark quasi-PDF.

- L.-B. Chen, R.-L. Zhu and W. Wang, PRL126 (2021);
- Z.-Y. Li, Y.-Q. Ma and J.-W. Qiu, PRL126 (2021).

- Matching coefficient:

$$C^{(1)}\left(\xi, \frac{\mu}{yP^z}\right) = -\frac{\alpha_s C_F}{2\pi}\delta(1-\xi)\left[\frac{3}{2}\ln\frac{\mu^2}{4x^2P_z^2} + \frac{5}{2}\right]$$

$\xi = \frac{x}{y}$

$$-\frac{\alpha_s C_F}{2\pi}\begin{cases} \left(\frac{1+\xi^2}{1-\xi}\ln\frac{\xi}{\xi-1} + 1\right)_+ & \xi > 1 \\ \left(\frac{1+\xi^2}{1-\xi}\left[-\ln\frac{\mu^2}{y^2P_z^2} + \ln\left(4\xi(1-\xi)\right) - 1\right] + 1\right)_+ & 0 < \xi < 1 \\ \left(-\frac{1+\xi^2}{1-\xi}\ln\frac{-\xi}{1-\xi} - 1\right)_+ & \xi < 0 \end{cases}$$

Precision calculation of the x-dependence of PDFs

- Large-momentum expansion:

$$f(x,\mu) = \int_{-\infty}^{\infty} \frac{dy}{|y|} C\left(\frac{x}{y}, \frac{\mu}{yP^z}\right) \tilde{f}(y, P^z, \mu) + \mathcal{O}\left(\frac{\Lambda_{\rm QCD}^2}{(xP^z)^2}, \frac{\Lambda_{\rm QCD}^2}{((1-x)P^z)^2}\right)$$

State-of-the-art: next-to-next-to-leading order (NNLO) matching for the non-singlet quark quasi-PDF.

- L.-B. Chen, R.-L. Zhu and W. Wang, PRL126 (2021);
- Z.-Y. Li, Y.-Q. Ma and J.-W. Qiu, PRL126 (2021).

- Matching coefficient:

$$\ln\frac{\mu^2}{y^2P_z^2} = \ln\frac{\mu^2}{x^2P_z^2} + \ln\frac{x^2}{y^2}$$

$$C^{(1)}\left(\xi, \frac{\mu}{yP^z}\right) = -\frac{\alpha_s C_F}{2\pi}\delta(1-\xi)\left[\frac{3}{2}\ln\frac{\mu^2}{4x^2P_z^2} + \frac{5}{2}\right]$$

$$\xi = \frac{x}{y}$$

$$-\frac{\alpha_s C_F}{2\pi}\begin{cases} \left(\frac{1+\xi^2}{1-\xi}\ln\frac{\xi}{\xi-1} + 1\right)_+ & \xi > 1 \\ \left(\frac{1+\xi^2}{1-\xi}\left[-\ln\frac{\mu^2}{y^2P_z^2} + \ln\left(4\xi(1-\xi)\right) - 1\right] + 1\right)_+ & 0 < \xi < 1 \\ \left(-\frac{1+\xi^2}{1-\xi}\ln\frac{-\xi}{1-\xi} - 1\right)_+ & \xi < 0 \end{cases}$$

Similar to DGLAP evolution:

$$\frac{dC(\xi, \mu/(xP^z))}{d\ln(xP^z)} = \frac{\alpha_s C_F}{\pi}\left[P_{qq}^{(0)}(\xi) - \frac{3}{2}\delta(1-\xi)\right]$$

X. Ji, Y.-S. Liu, Y. Liu, J.-H. Zhang and YZ, arXiv: 2004.03543.

Precision calculation of the x-dependence of PDFs

- Large-momentum expansion:

$$f(x,\mu) = \int_{-\infty}^{\infty} \frac{dy}{|y|} C\left(\frac{x}{y}, \frac{\mu}{yP^z}\right) \tilde{f}(y, P^z, \mu) + \mathcal{O}\left(\frac{\Lambda_{\rm QCD}^2}{(xP^z)^2}, \frac{\Lambda_{\rm QCD}^2}{((1-x)P^z)^2}\right)$$

State-of-the-art: next-to-next-to-leading order (NNLO) matching for the non-singlet quark quasi-PDF.

- L.-B. Chen, R.-L. Zhu and W. Wang, PRL126 (2021);
- Z.-Y. Li, Y.-Q. Ma and J.-W. Qiu, PRL126 (2021).

- Matching coefficient:

$$C^{(1)}\left(\xi, \frac{\mu}{yP^z}\right) = -\frac{\alpha_s C_F}{2\pi}\delta(1-\xi)\left[\frac{3}{2}\ln\frac{\mu^2}{4x^2P_z^2} + \frac{5}{2}\right]$$

$\xi = \frac{x}{y}$

$$-\frac{\alpha_s C_F}{2\pi}\begin{cases} \left(\frac{1+\xi^2}{1-\xi}\ln\frac{\xi}{\xi-1} + 1\right)_+ & \xi > 1 \\ \left(\frac{1+\xi^2}{1-\xi}\left[-\ln\frac{\mu^2}{y^2P_z^2} + \ln\left(4\xi(1-\xi)\right) - 1\right] + 1\right)_+ & 0 < \xi < 1 \\ \left(-\frac{1+\xi^2}{1-\xi}\ln\frac{-\xi}{1-\xi} - 1\right)_+ & \xi < 0 \end{cases}$$

Precision calculation of the x-dependence of PDFs

- Large-momentum expansion:

$$f(x,\mu) = \int_{-\infty}^{\infty} \frac{dy}{|y|} C\left(\frac{x}{y}, \frac{\mu}{yP^z}\right) \tilde{f}(y, P^z, \mu) + \mathcal{O}\left(\frac{\Lambda^2_{\rm QCD}}{(xP^z)^2}, \frac{\Lambda^2_{\rm QCD}}{((1-x)P^z)^2}\right)$$

State-of-the-art: next-to-next-to-leading order (NNLO) matching for the non-singlet quark quasi-PDF.

- L.-B. Chen, R.-L. Zhu and W. Wang, PRL126 (2021);
- Z.-Y. Li, Y.-Q. Ma and J.-W. Qiu, PRL126 (2021).

- Matching coefficient:

$$C^{(1)}\left(\xi, \frac{\mu}{yP^z}\right) = -\frac{\alpha_s C_F}{2\pi}\delta(1-\xi)\left[\frac{3}{2}\ln\frac{\mu^2}{4x^2P_z^2} + \frac{5}{2}\right]$$

$$\xi = \frac{x}{y}$$

$$-\frac{\alpha_s C_F}{2\pi}\begin{cases} \left(\dfrac{1+\xi^2}{1-\xi}\ln\dfrac{\xi}{\xi-1} + 1\right)_+ \\ \left(\dfrac{1+\xi^2}{1-\xi}\left[-\ln\dfrac{\mu^2}{y^2P_z^2} + \ln\left(4\xi(1-\xi)\right) - 1\right] + 1\right)_+ & 0 < \xi < 1 \\ \left(-\dfrac{1+\xi^2}{1-\xi}\ln\dfrac{-\xi}{1-\xi} - 1\right)_+ & \xi < 0 \end{cases}$$

Threshold logarithms:

$$C(\xi, \mu/(yP^z)) \sim \frac{\alpha_s C_F}{2\pi}\left[\frac{2\ln|1-\xi|}{|1-\xi|} - \frac{2}{1-\xi}\ln\frac{\mu^2}{P_z^2} - \frac{2}{1-\xi}\right]_+$$

Large-x behavior of the extracted PDF is sensitive to the large threshold logarithms.

X. Gao, YZ et al., 2102.01101.

Systematic procedure in lattice calculation

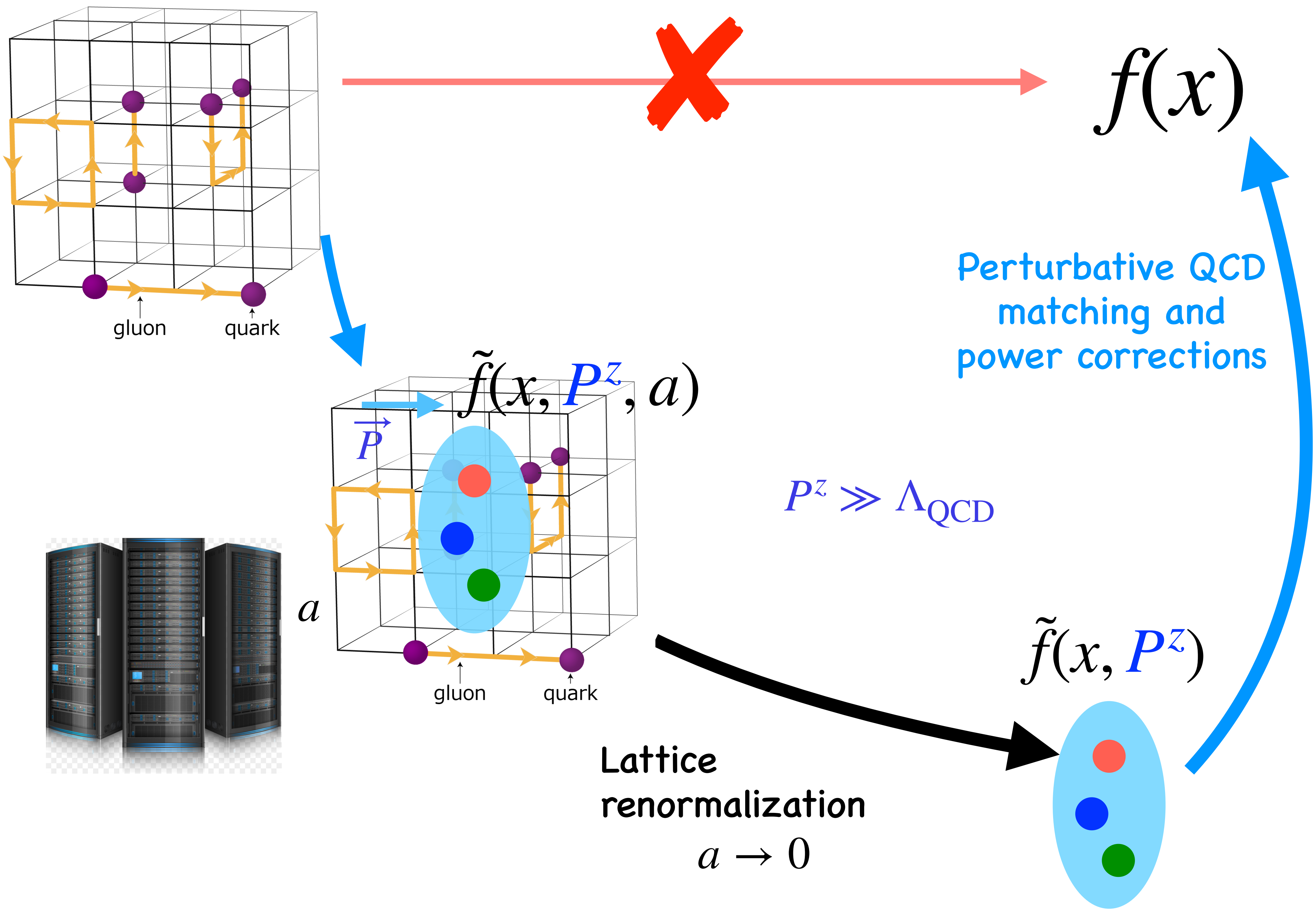

Encouraging results have been obtained so far:

For example, the isovector (u-d) PDFs of the proton, with RI/MOM lattice renormalization and NLO matching:

Helicity PDF

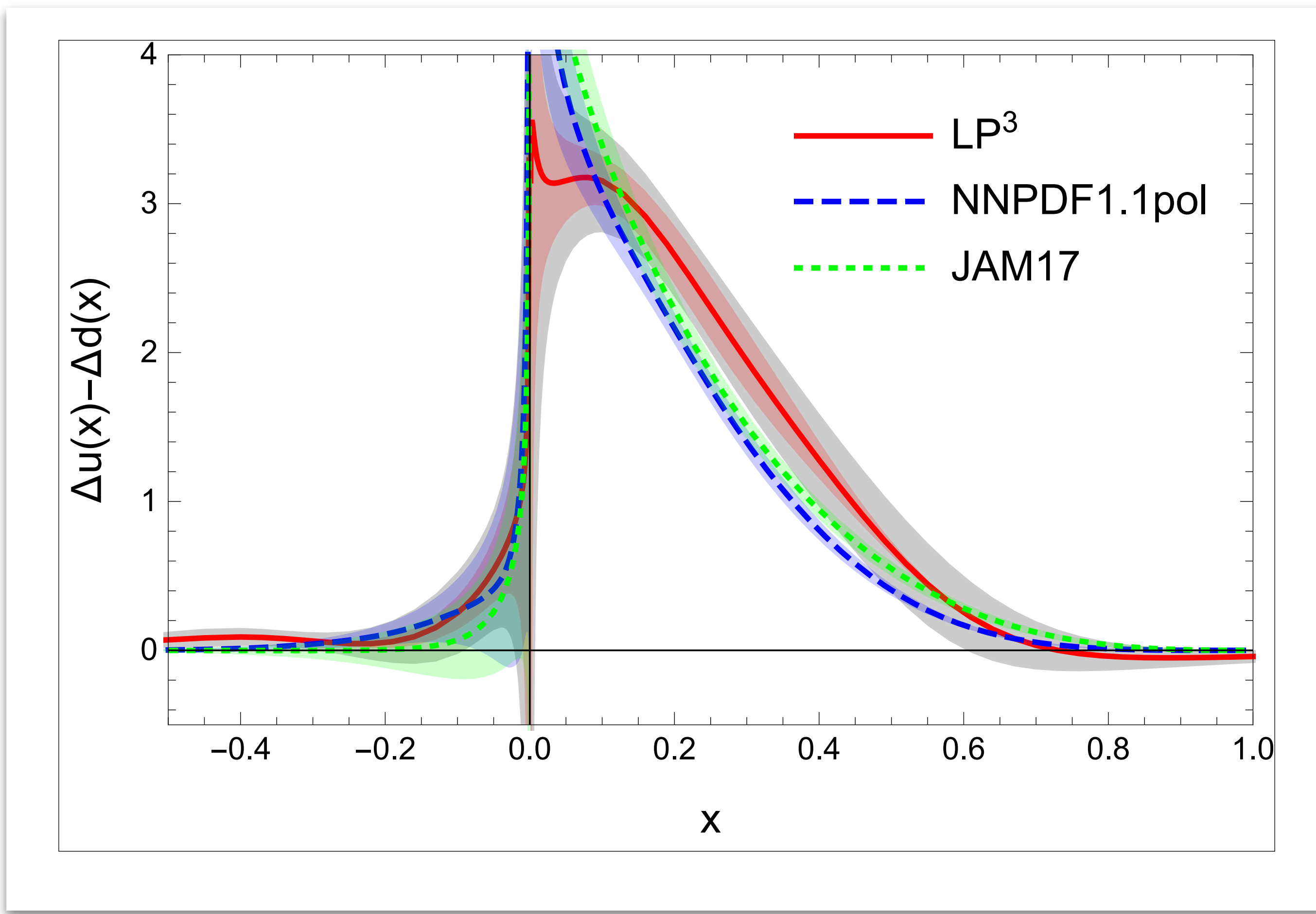

H.W. Lin, YZ, et al. (LP3 Collaboration), Phys.Rev.Lett. 121 (2018)

Transversity PDF

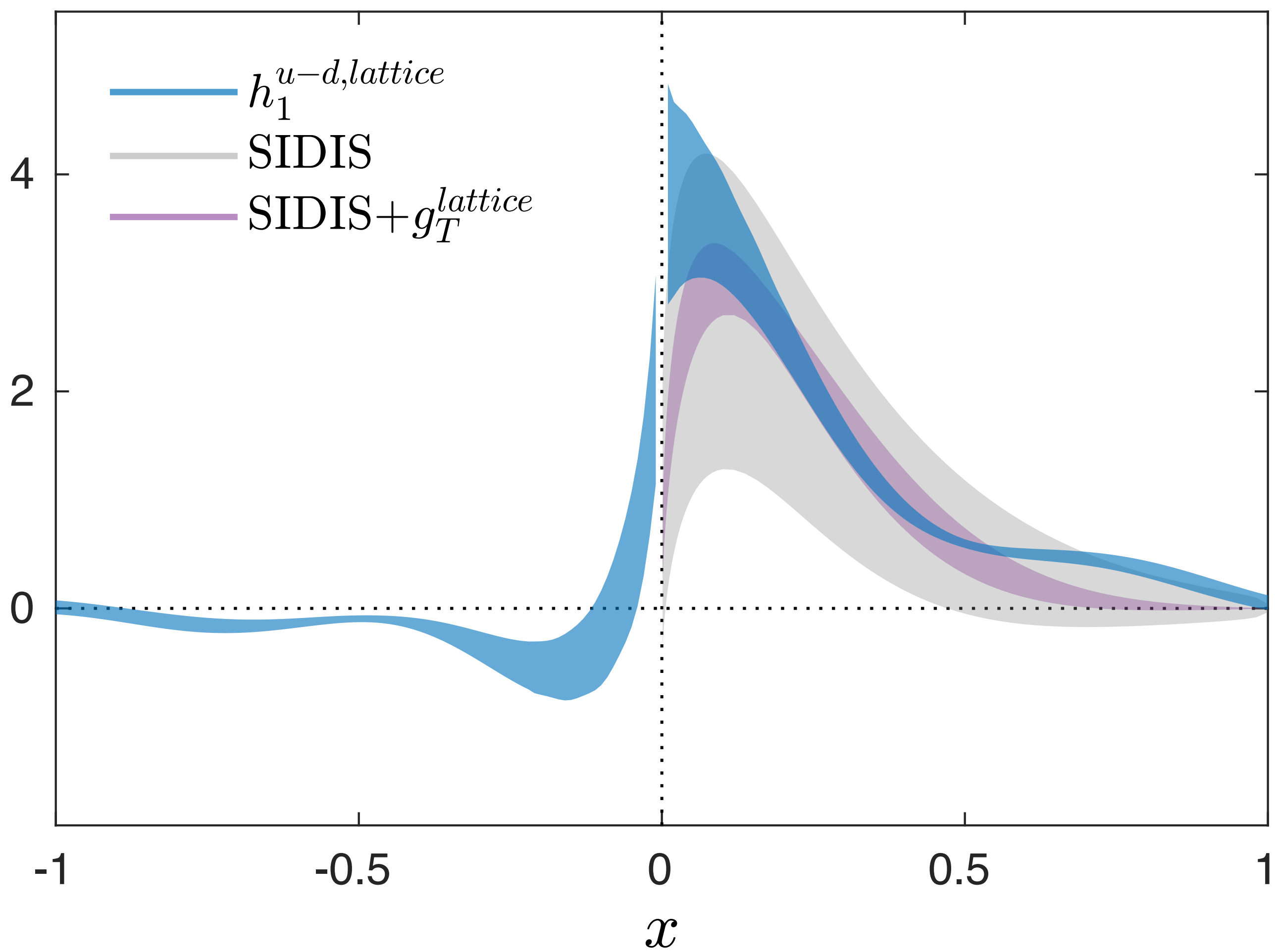

C. Alexandrou, et al. (ETM), Phys.Rev.D 98 (2018).

Encouraging results have been obtained so far:

For example, the isovector (u-d) PDFs of the proton, with RI/MOM lattice renormalization and NLO matching:

Helicity PDF

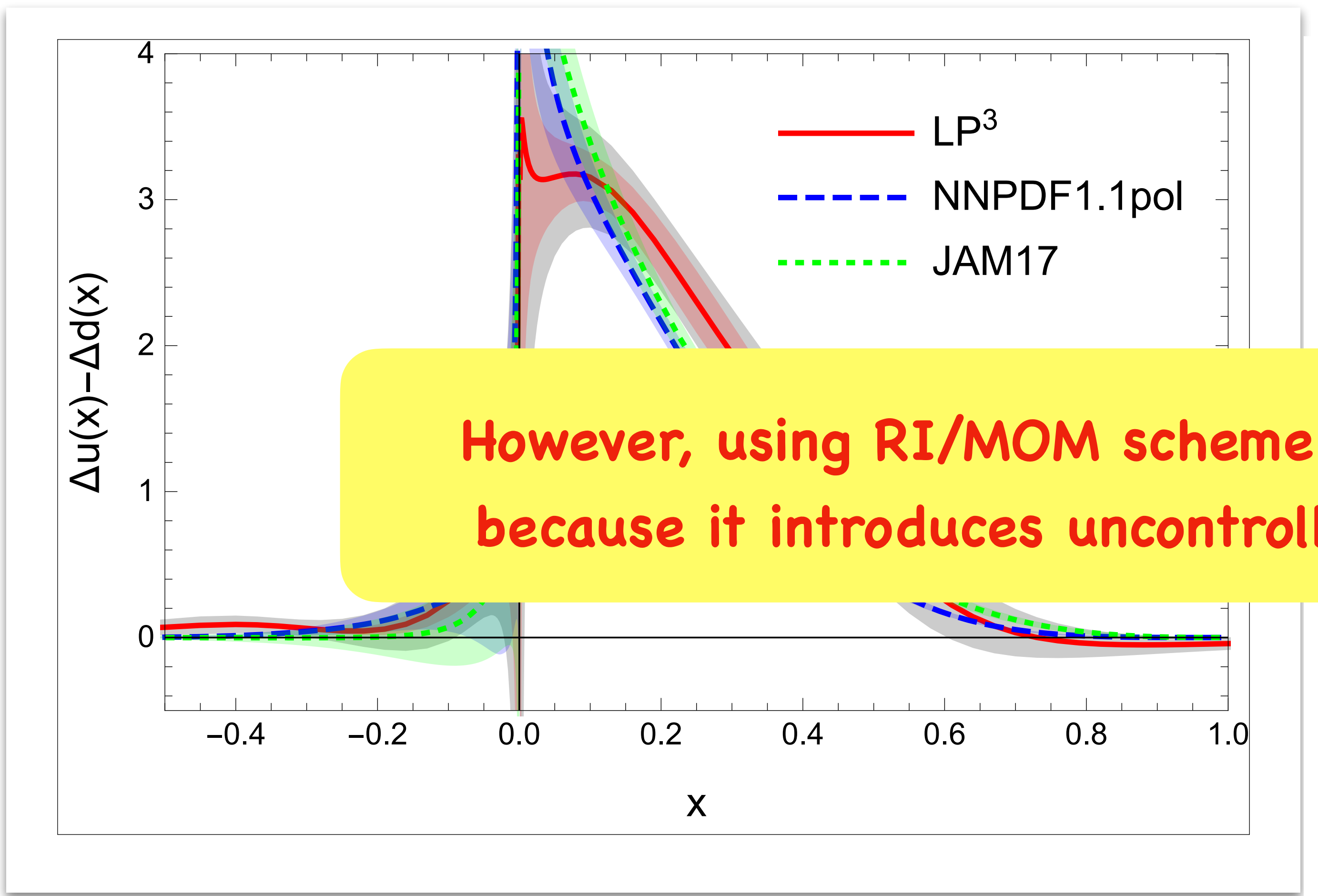

Transversity PDF

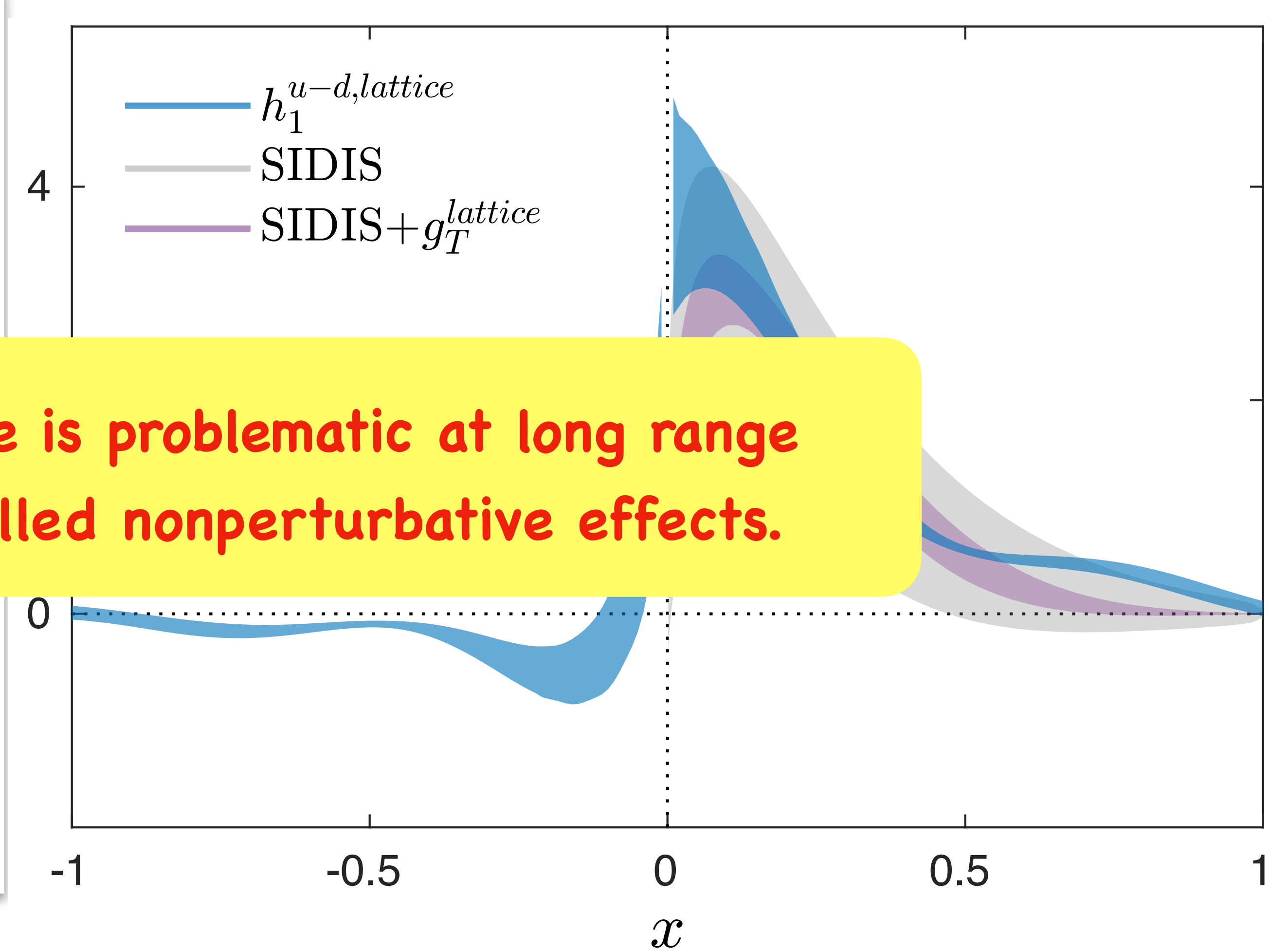

However, using RI/MOM scheme is problematic at long range because it introduces uncontrolled nonperturbative effects.

H.W. Lin, YZ, et al. (LP3 Collaboration), Phys.Rev.Lett. 121 (2018)

C. Alexandrou, et al. (ETM), Phys.Rev.D 98 (2018).

Hybrid scheme (controlling the power corrections)

$$O^{\Gamma}_{B}(z,a) = \bar{\psi}_0(z)\Gamma W_0[z,0]\psi_0(0) = e^{\delta m|z|}\, Z_{j_1}(a) Z_{j_2}(a) O^{\Gamma}_{R}(z)$$

See X. Ji, YZ, et al., NPB 964 (2021) and references therein.

$$\tilde{h}(z, P^z) = \langle P | O(z,\mu) | P \rangle$$

A "minimal" subtraction:

- Wilson-line mass subtraction δm;

$$O^{\Gamma}_{R}(z,\mu_R) = Z_{\text{hybrid}}(a,\mu_R) e^{-\delta m|z|} O^{\Gamma}_{B}(z,a)$$

- Overall renormalization Z_j's.

Ratio-type schemes:

- RIMOM

$$Z_X = \langle q | O^{\Gamma}(z) | q \rangle$$

- Hadron matrix elements

$$Z_X = \langle P^z_0 = 0 | O^{\Gamma}(z) | P^z_0 = 0 \rangle$$

- Vacuum expectation value

$$Z_X = \langle \Omega | O^{\Gamma}(z) | \Omega \rangle$$

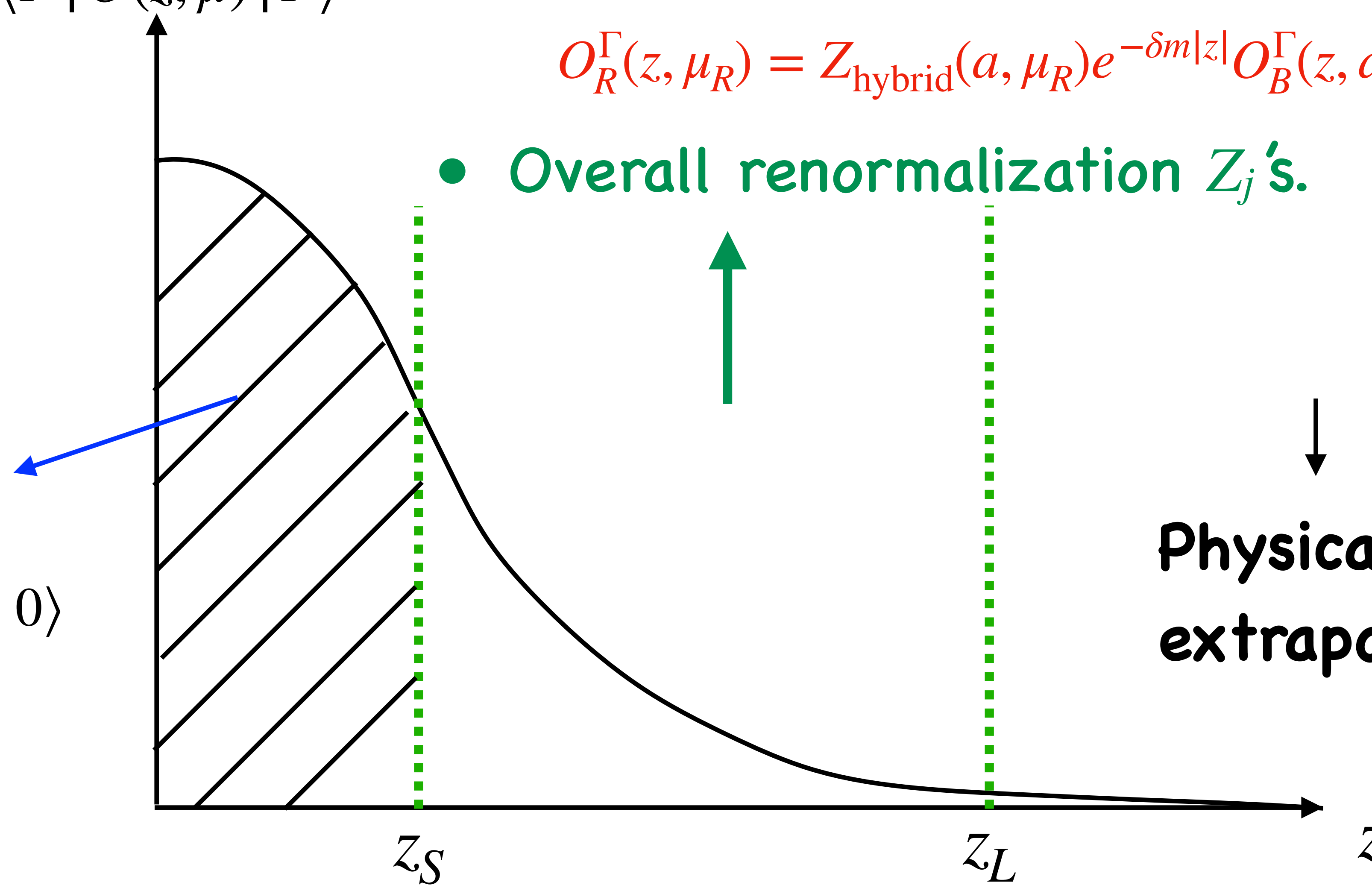

Physical extrapolation

$a \ll z_S \ll \Lambda^{-1}_{\text{QCD}}$

$z_L \sim \Lambda^{-1}_{\text{QCD}}$

Hybrid scheme (controlling the power corrections)

$$O_B^{\Gamma}(z,a) = \bar{\psi}_0(z)\Gamma W_0[z,0]$$

See X. Ji, YZ, et al., NPB 964 (2021) and references therein.

$$\tilde{h}(z,P^z) = \langle P|O(z,\mu)|P\rangle$$

Coordinate-Space Factorization (or OPE):

$$\tilde{h}(\lambda = zP^z, z^2\mu^2) = \int_0^1 d\alpha\ \mathscr{C}(\alpha, z^2\mu^2)\ h(\alpha\lambda,\mu) + \mathcal{O}(z^2\Lambda^2_{\rm QCD})$$

$$\tilde{h}(\lambda = zP^z, z^2\mu^2) = \sum_{n=0}^{\infty} \frac{(-i\lambda)^n}{n!} C_n\left(z^2\mu^2\right) a_n(\mu) + \mathcal{O}(z^2\Lambda^2_{\rm QCD})$$

Suitable for calculating moments or model fitting of the PDFs.

"Ioffe-time distribution", Radyushkin, Phys.Rev.D 96 (2017); **Current-current correlator**, Braun and Mueller, EPJC 55 (2008); Ma and Qiu, PRL120 (2018).

Ratio-type schemes:

- RIMOM

$$Z_X = \langle q|O^{\Gamma}(z)|q\rangle$$

- Hadron matrix elements

$$Z_X = \langle P_0^z = 0|O^{\Gamma}(z)|P_0^z = 0\rangle$$

- Vacuum expectation value

$$Z_X = \langle \Omega|O^{\Gamma}(z)|\Omega\rangle$$

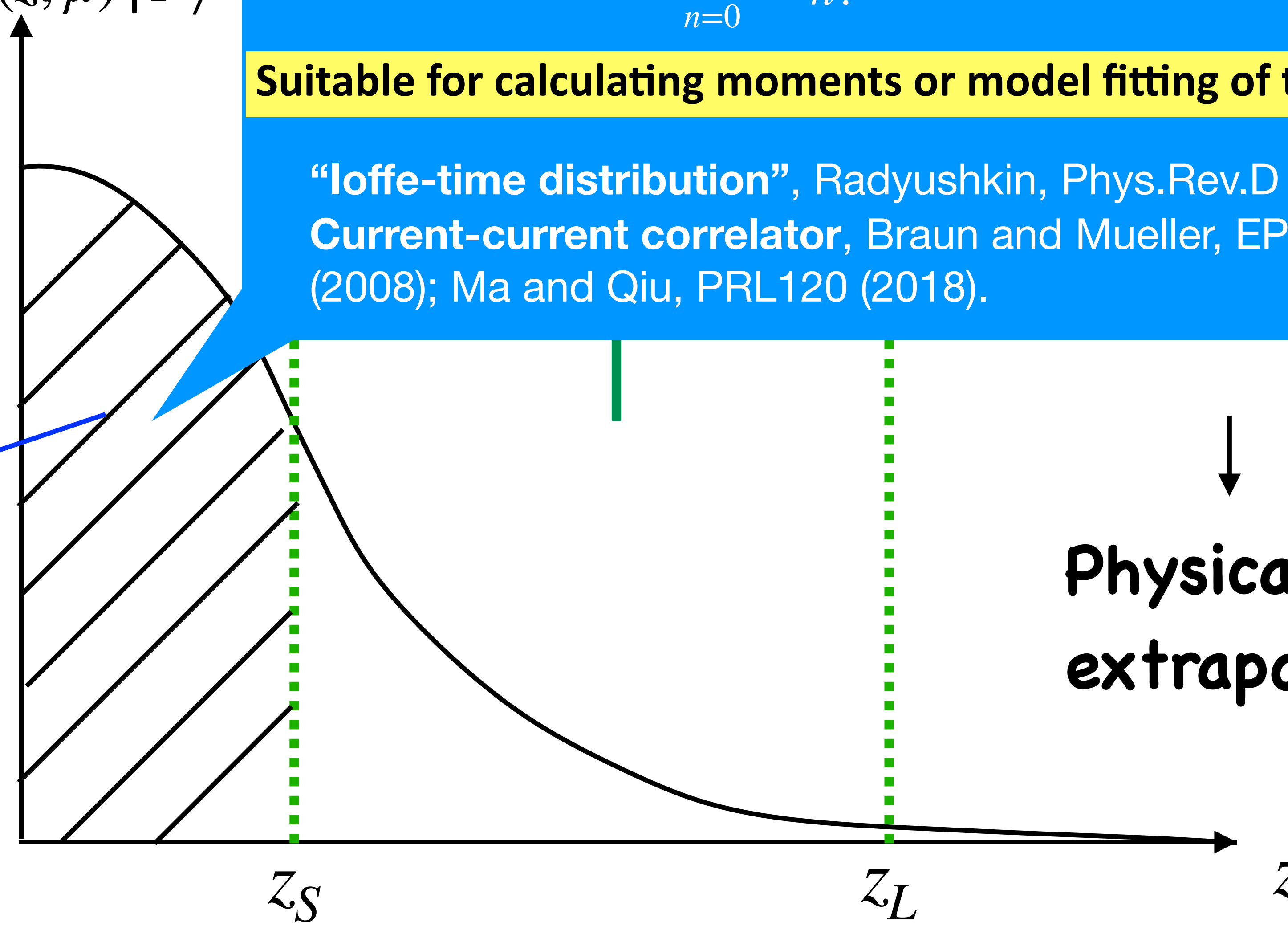

$a \ll z_S \ll \Lambda^{-1}_{\rm QCD}$

$z_L \sim \Lambda^{-1}_{\rm QCD}$

Physical extrapolation

Lattice data

- Wilson-clover fermion on 2+1 flavor HISQ configurations.

n_z	P_z (GeV)		ζ
	$a = 0.06$ fm	$a = 0.04$ fm	
0	0	0	0
1	0.43	0.48	0
2	0.86	0.97	1
3	1.29	1.45	2/3
4	1.72	1.93	3/4
5	2.15	2.42	3/5

$48^3 \times 64$ $\quad$ $64^3 \times 64$

$m_\pi = 300$ MeV

$a = 0.076$ fm

$P_z = 0$ GeV, 0.25 GeV, 0.51 GeV, 0.76 GeV, 1.02 GeV, 1.27 GeV, 1.53 GeV, 1.78 GeV, 2.04 GeV, 2.29 GeV

$64^3 \times 64$

$m_\pi = 140$ MeV

- X. Gao, YZ, et al., PRD102 (2020).
- X. Gao, YZ, et al., 2102.01101.

Wilson-line mass renormalization

- Polyakov loop

$\langle\Omega|$ 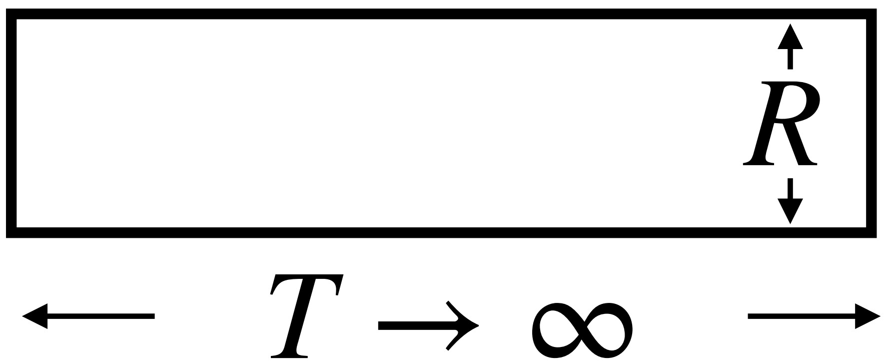 $|\Omega\rangle \;\propto \exp[-V(R)T]$

- Renormalization condition:

$$V^{\rm lat}(r,a)\Big|_{r=r_0} + 2\delta m(a) = 0.95/r_0$$

$$\delta m(a) = \frac{1}{a}\sum_n c_n \alpha_s^n(1/a) + \delta m_0^{\rm lat}$$

$$\delta m_0^{\rm lat} \sim \Lambda_{\rm QCD}$$

C. Bauer, G. Bali and A. Pineda, PRL108 (2012).

$$a\delta m(a = 0.04\ \text{fm}) = 0.1508(12)$$

$$a\delta m(a = 0.06\ \text{fm}) = 0.1586(8)$$

$$a\delta m(a = 0.076\ \text{fm}) = 0.1597(16)$$

A. Bazavov et al., TUMQCD, PRD98 (2018).

Wilson-line mass renormalization

- Check of continuum limit:

$$O_B^{\Gamma}(z,a) = e^{\delta m|z|}\, Z_{j_1}(a)Z_{j_2}(a)O_R^{\Gamma}(z)$$

$$\lim_{a\to 0} e^{-\delta m(z-z_0)}\frac{\tilde{h}(z,a,P^z=0)}{\tilde{h}(z_0,a,P^z=0)} = \frac{\tilde{h}(z,P^z=0,\ \mu)}{\tilde{h}(z_0,P^z=0,\ \mu)} \qquad z, z_0 \gg a$$

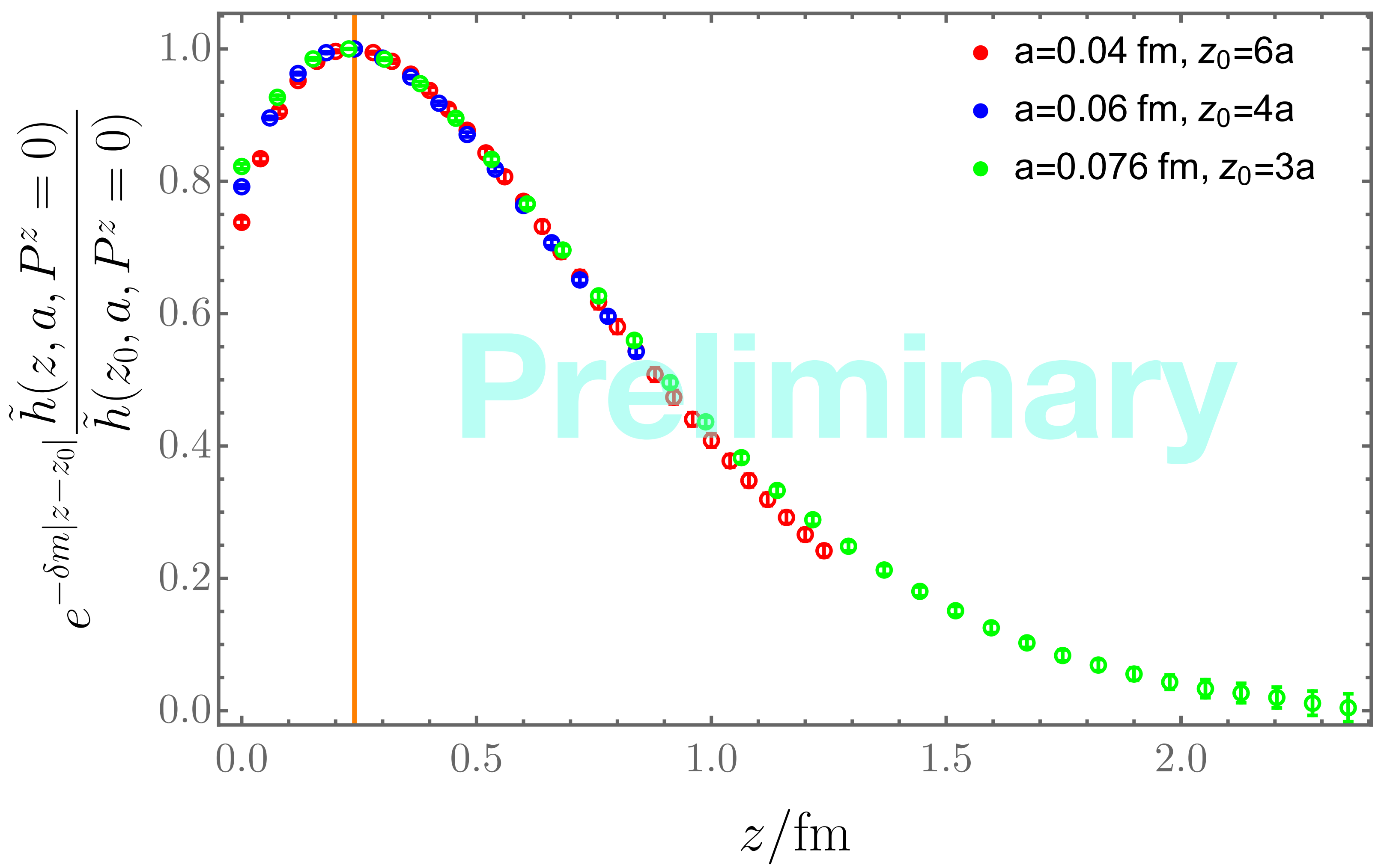

Wilson-line mass renormalization

- Matching to the MSbar scheme:

$$e^{\delta m_0^{\overline{\rm MS}}(z-z_0)} \lim_{a\to 0} e^{-\delta m(z-z_0)} \frac{\tilde h(z, a, P^z=0)}{\tilde h(z_0, a, P^z=0)} = \frac{\tilde h(z, P^z=0,\ \mu)}{\tilde h(z_0, P^z=0,\ \mu)} \qquad z, z_0 \gg a$$

Renormalon in the Wilson-line mass correction.

C. Bauer, G. Bali and A. Pineda, PRL108 (2012);
C. Alexandrou et al. (ETMC), 2011.00964.

$$\tilde h^{\overline{\rm MS}}(z, P^z=0,\ \mu) = C_0(\alpha_s(\mu), z^2\mu^2) + \mathcal{O}(z^2\Lambda_{\rm QCD}^2) \qquad z \ll \Lambda_{\rm QCD}^{-1}$$

Perturbative:

- Known to NNLO
  - L.-B. Chen, R.-L. Zhu and W. Wang, PRL126 (2021);
  - Z.-Y. Li, Y.-Q. Ma and J.-W. Qiu, PRL126 (2021).
- 3-loop anomalous dimension available.
  - V. Braun and K. G. Chetyrkin, JHEP 07 (2020).

Non-perturbative:

- Leading infrared renormalon contribution is quadratic $\propto z^2\Lambda_{\rm QCD}^2$
  - V. Braun, A. Vladimirov and J.-H. Zhang, PRD99 (2019).

Wilson-line mass renormalization

- Matching to the MSbar scheme:

$$e^{-\delta m(z-z_0)} \frac{\tilde{h}(z, a, P^z = 0)}{\tilde{h}(z_0, a, P^z = 0)} = e^{-\delta m_0^{\overline{\rm MS}}(z-z_0)} \frac{C_0(\alpha_s(\mu), z^2\mu^2) + \Lambda z^2}{C_0(\alpha_s(\mu), z_0^2\mu^2) + \Lambda z_0^2} \qquad z_0 \gg a$$

  - Use both fixed-order and renormalization-group improved (RGI) NNLO OPE formulae;

X. Gao, YZ et al., 2102.01101.

  - Two parameter fit to a wide range of z.

Wilson-line mass renormalization

- Matching to the MSbar scheme:
  - Fixed-order OPE leads to excellent fits, while RGI OPE does not;
  - The a-dependences of the parameters are negligible.

	$z_{\rm max} = 0.48$ fm	$z_{\rm max} = 0.60$ fm	$z_{\rm max} = 0.72$ fm
$a = 0.04$ fm, $\mu = 2.0$ GeV	$\chi^2_{dof} = 0.33$, $\delta m_0 \to 0.166$, $\Lambda \to -0.0475$	$\chi^2_{dof} = 0.26$, $\delta m_0 \to 0.164$, $\Lambda \to -0.0485$	$\chi^2_{dof} = 0.45$, $\delta m_0 \to 0.167$, $\Lambda \to -0.0472$
$a = 0.06$ fm, $\mu = 2.0$ GeV	$\chi^2_{dof} = 0.0015$, $\delta m_0 \to 0.169$, $\Lambda \to -0.0485$	$\chi^2_{dof} = 0.024$, $\delta m_0 \to 0.173$, $\Lambda \to -0.0468$	$\chi^2_{dof} = 0.24$, $\delta m_0 \to 0.179$, $\Lambda \to -0.044$
	$z_{\rm max} = 0.532$ fm	$z_{\rm max} = 0.608$ fm	$z_{\rm max} = 0.684$ fm
$a = 0.076$ fm, $\mu = 2.0$ GeV	$\chi^2_{dof} = 0.011$, $\delta m_0 \to 0.171$, $\Lambda \to -0.0449$	$\chi^2_{dof} = 0.11$, $\delta m_0 \to 0.174$, $\Lambda \to -0.0436$	$\chi^2_{dof} = 0.38$, $\delta m_0 \to 0.178$, $\Lambda \to -0.0421$

Preliminary

Table 4: δm_0 in unit of GeV, Λ in unit of GeV^2, and λ in unit of GeV^4.

$z_0 = 4a$

Physical extrapolation beyond z_L

- Space-like correlations have correlation length $\xi_z \sim 1/\Lambda_{\rm QCD}$. In $\lambda = zP^z$ space, the correlation length $\xi_\lambda = P^z\xi_z \sim P^z/\Lambda_{\rm QCD}$.
- As $P^z \to \infty$, $\xi_\lambda \to \infty$, only the twist-2 contribution remains, and the correlation decreases algebraically as $\sim 1/\lambda^d$ (Regge-like).

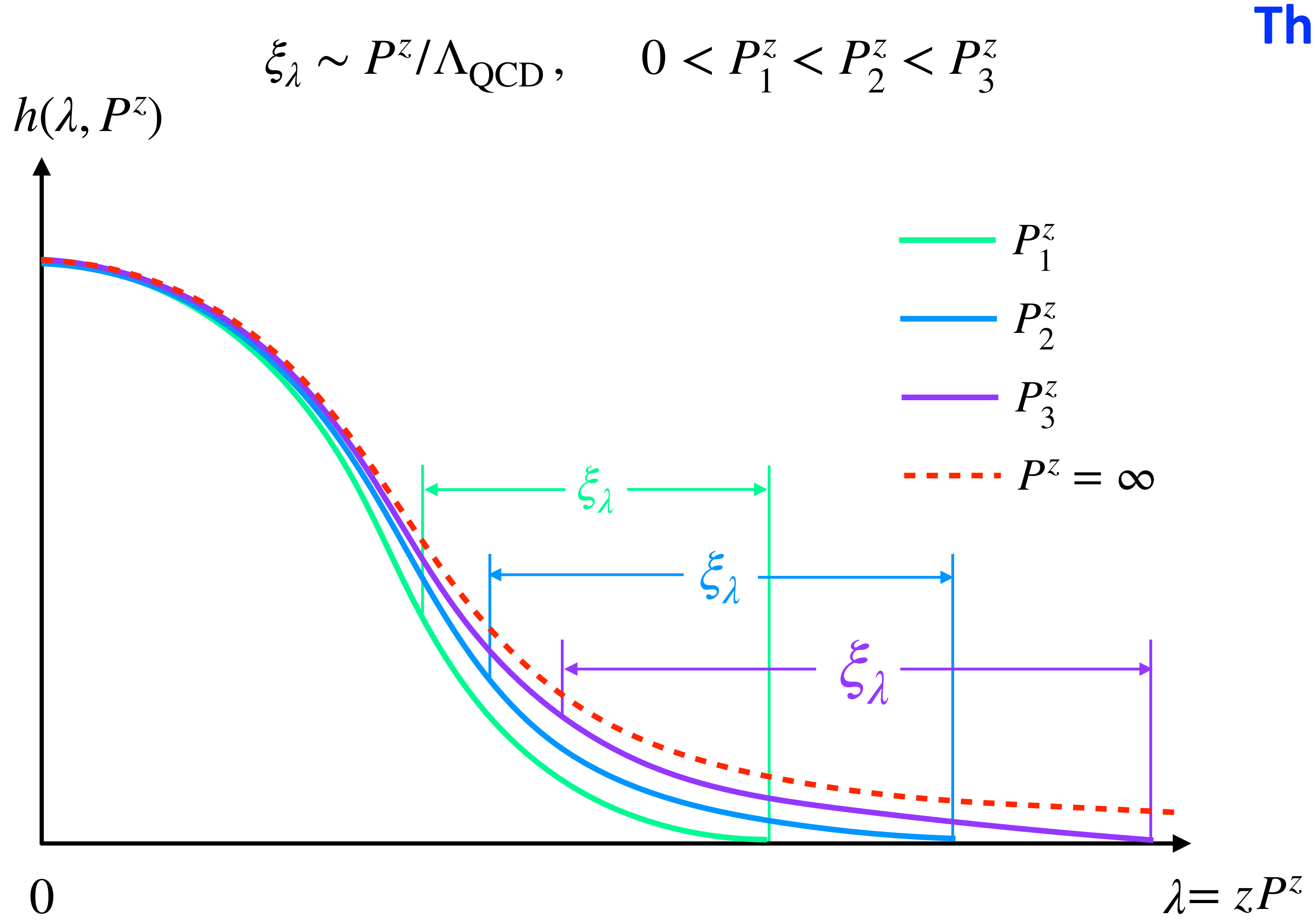

Therefore, if

P^z is not very large, e.g. 2–5 GeV for the proton:

- z_L or λ_L must be large enough for us to see the exponential decay;
- We can use an exponential-based form to extrapolate to ∞;

P^z is very large:

- Correlation is dominated by the leading-twist contribution;
- We can use an algebraic form to do the extrapolation.

Physical extrapolation beyond z_L

Impact of extrapolation:

- Remove unphysical oscillation from Fourier transform;
- The small-x region $x < 1/\lambda_L$ becomes model dependent. After all, LaMET can only predict$x \in [x_{\min}, x_{\max}]$ where usually $x_{\min} > 1/\lambda_L$.

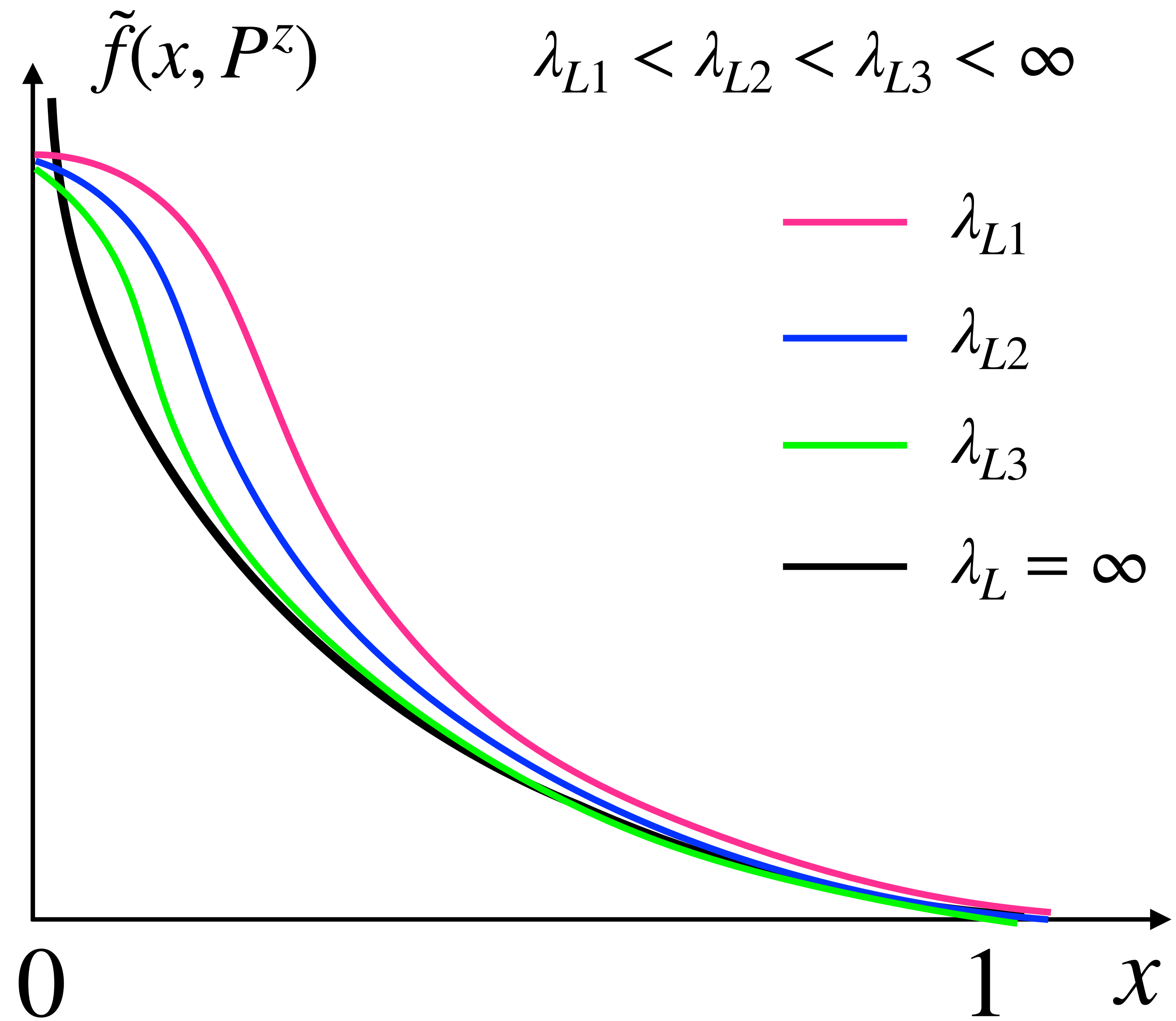

Implementation of the hybrid scheme

- Taking advantage of the fact that the NNLO OPE with leading IR renormalon contribution can fit to a wide range of z:

$$\lim_{a\to 0}\frac{\tilde{h}(z,a,P^z)}{\tilde{h}(z,a,P^z=0)}=\frac{\tilde{h}(z,P^z,\ \mu)}{\tilde{h}(z,P^z=0,\ \mu)}=\frac{\tilde{h}(z,P^z,\ \mu)}{C_0(\alpha_s(\mu),z^2\mu^2)+\Lambda z^2}$$

$$\downarrow$$

$$\lim_{a\to 0}\frac{\tilde{h}(z,a,P^z)}{\tilde{h}(z,a,P^z=0)}\frac{C_0(\alpha_s(\mu),z^2\mu^2)+\Lambda z^2}{C_0(\alpha_s(\mu),z^2\mu^2)}=\frac{\tilde{h}(z,P^z,\ \mu)}{C_0(\alpha_s(\mu),z^2\mu^2)}$$

Rigorous ratio scheme in

- T. Izubuchi, X. Ji, L. Jin, I. Stewart, and YZ, PRD98 (2018);

as compared to the original ratio in

- A. Radyushkin, Phys.Lett.B 781 (2018).

Fourier transform with physical extrapolation

- Extrapolation with models featuring an exponential decay:

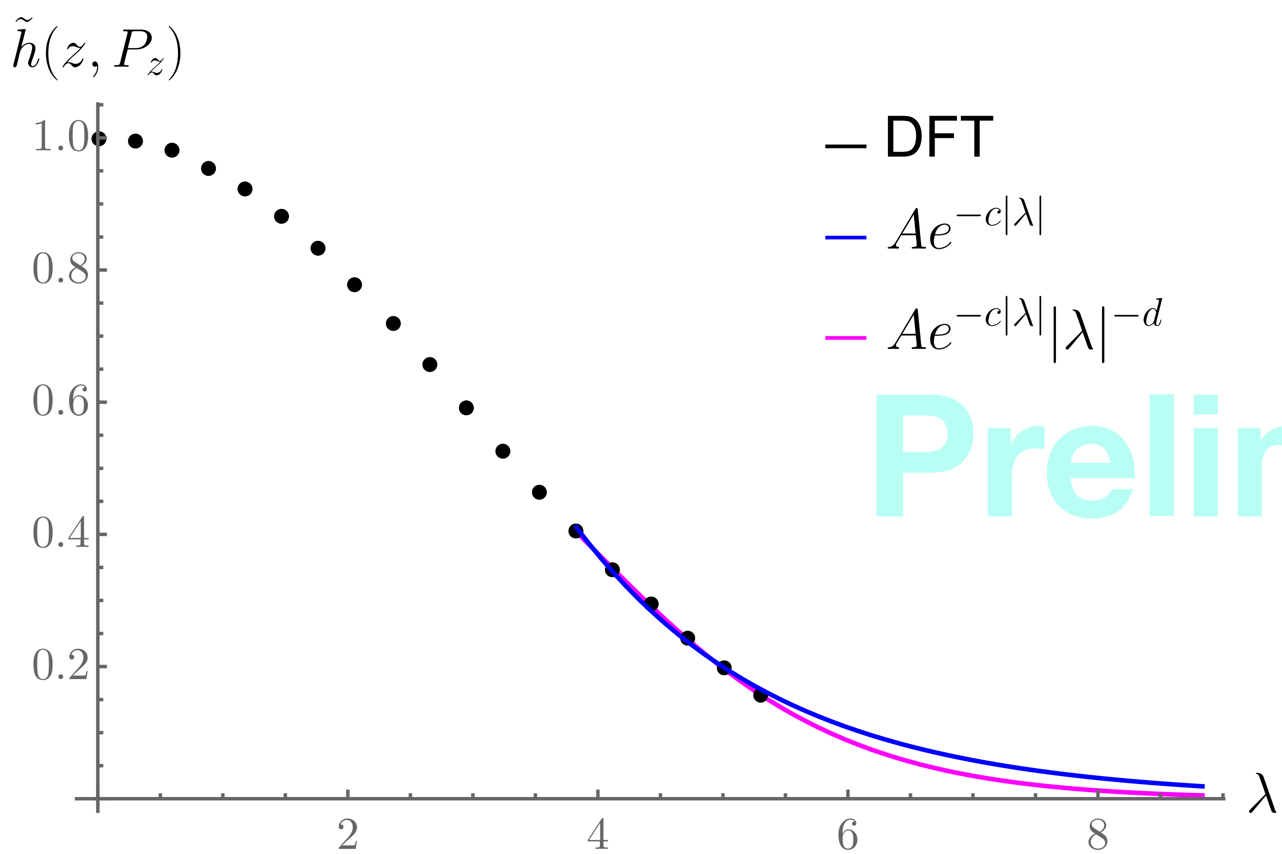

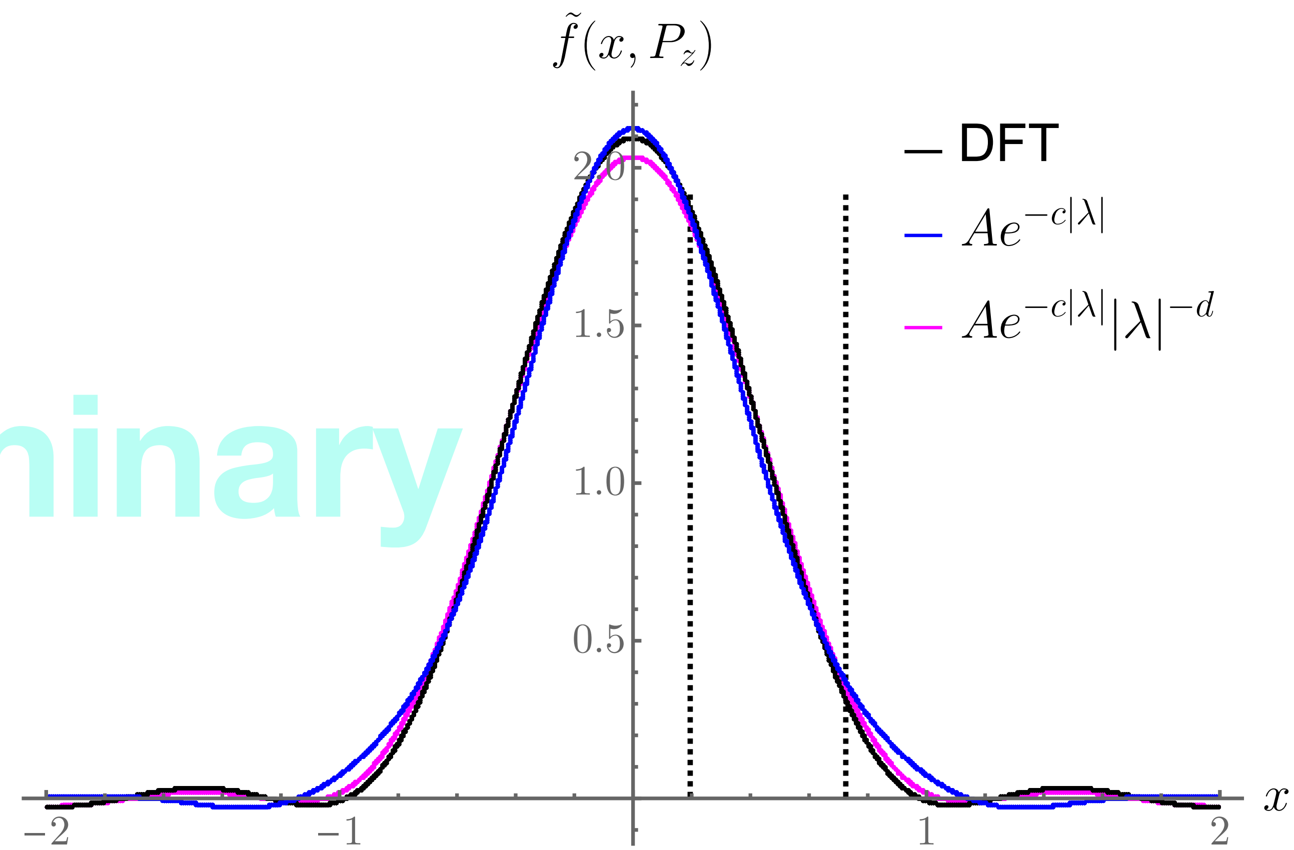

$\lambda = zP^z$ $\quad a = 0.04$ fm, $P_z = 1.45$ GeV, $z_S = 6a$, $z_L = 19a$.

Extrapolation barely affects the moderate x region, as expected.

Caveat: we are still in the process of finishing the hybrid-scheme analysis. In this talk we choose z_S=z_L<=0.72 fm for now. But strictly speaking, the factorization is in doubt at large z.

Perturbative matching at NNLO

- Perturbative correction shows good convergence.

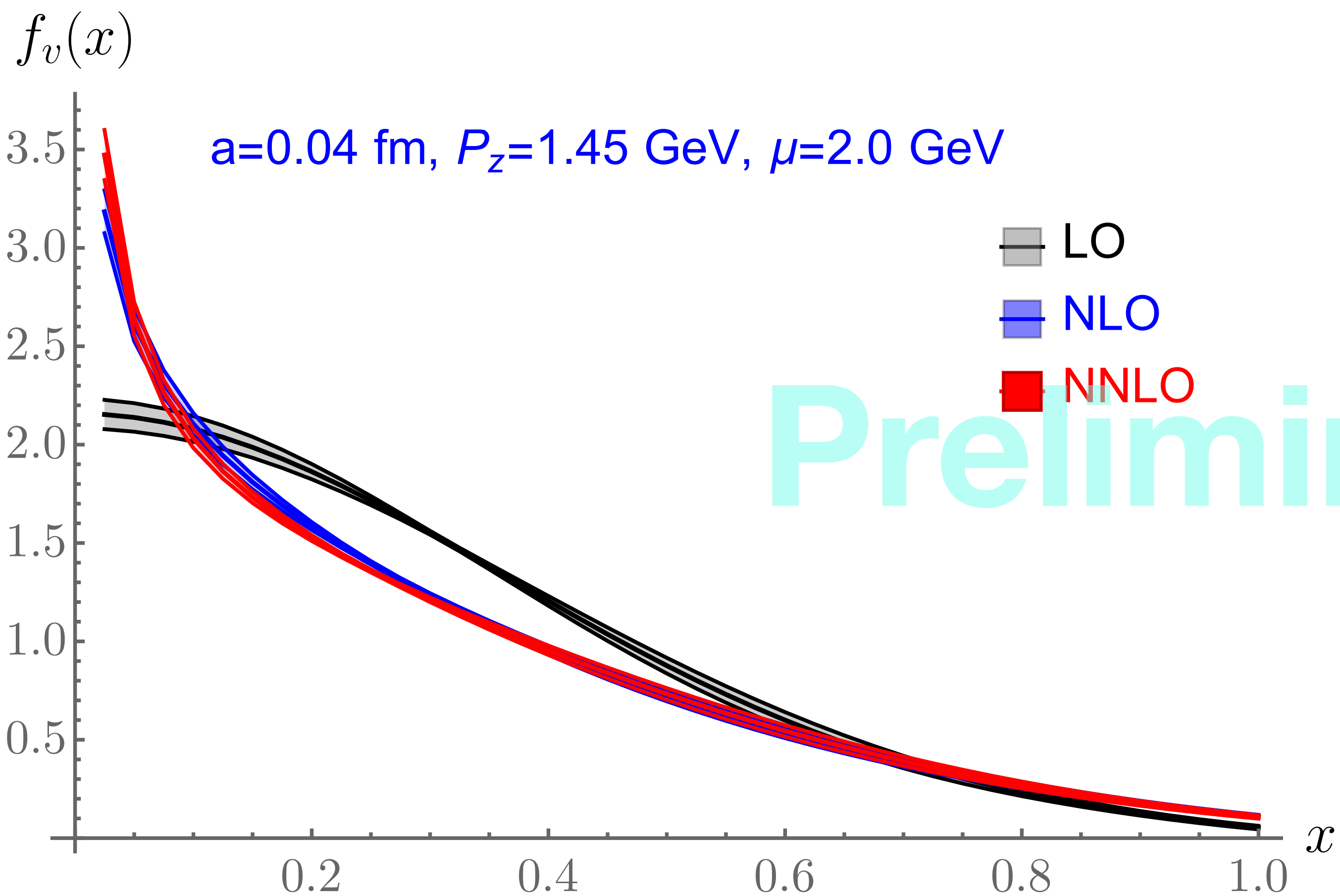

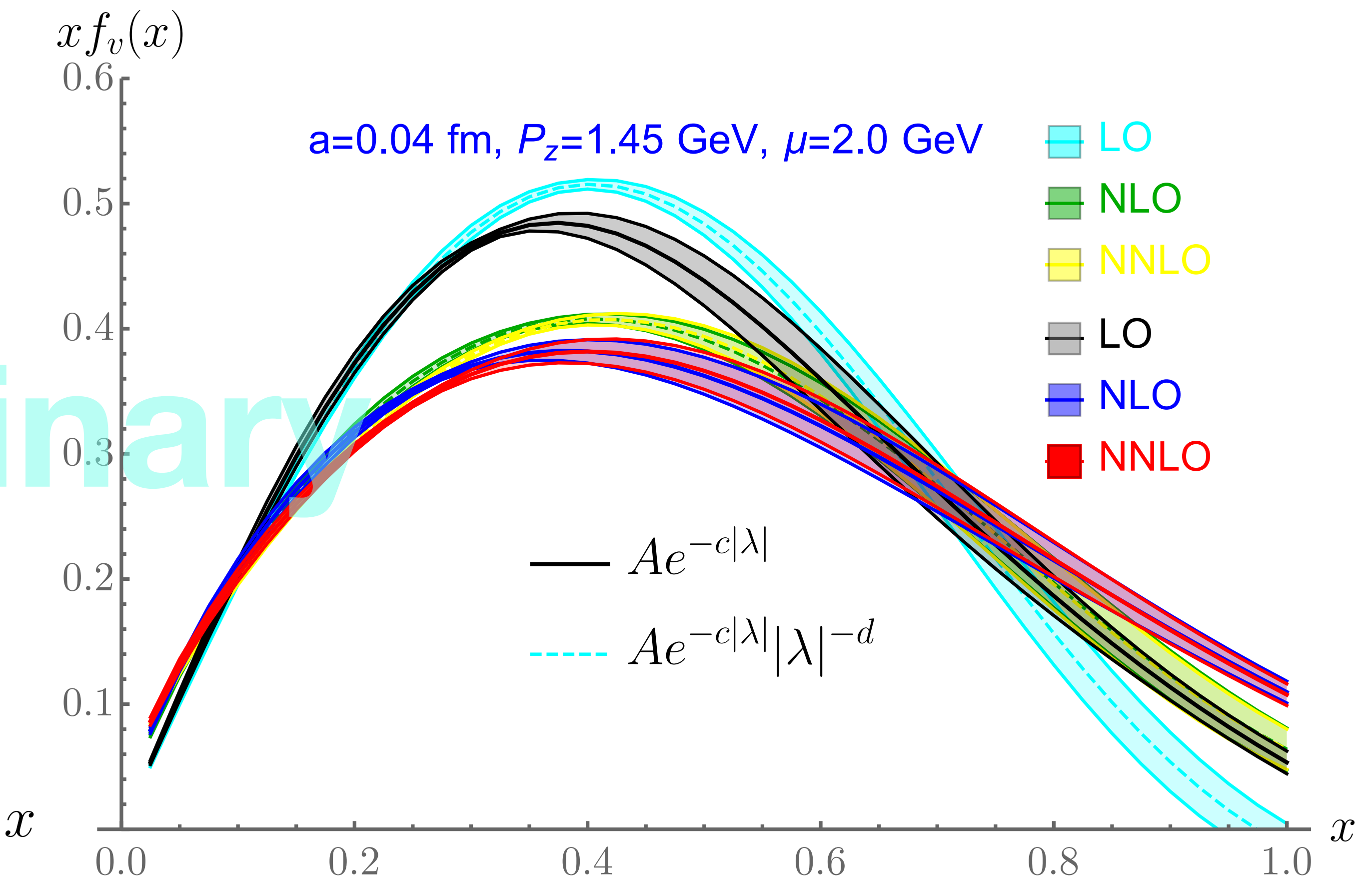

Error band only includes statistical uncertainty.

Dependence on P_z and a

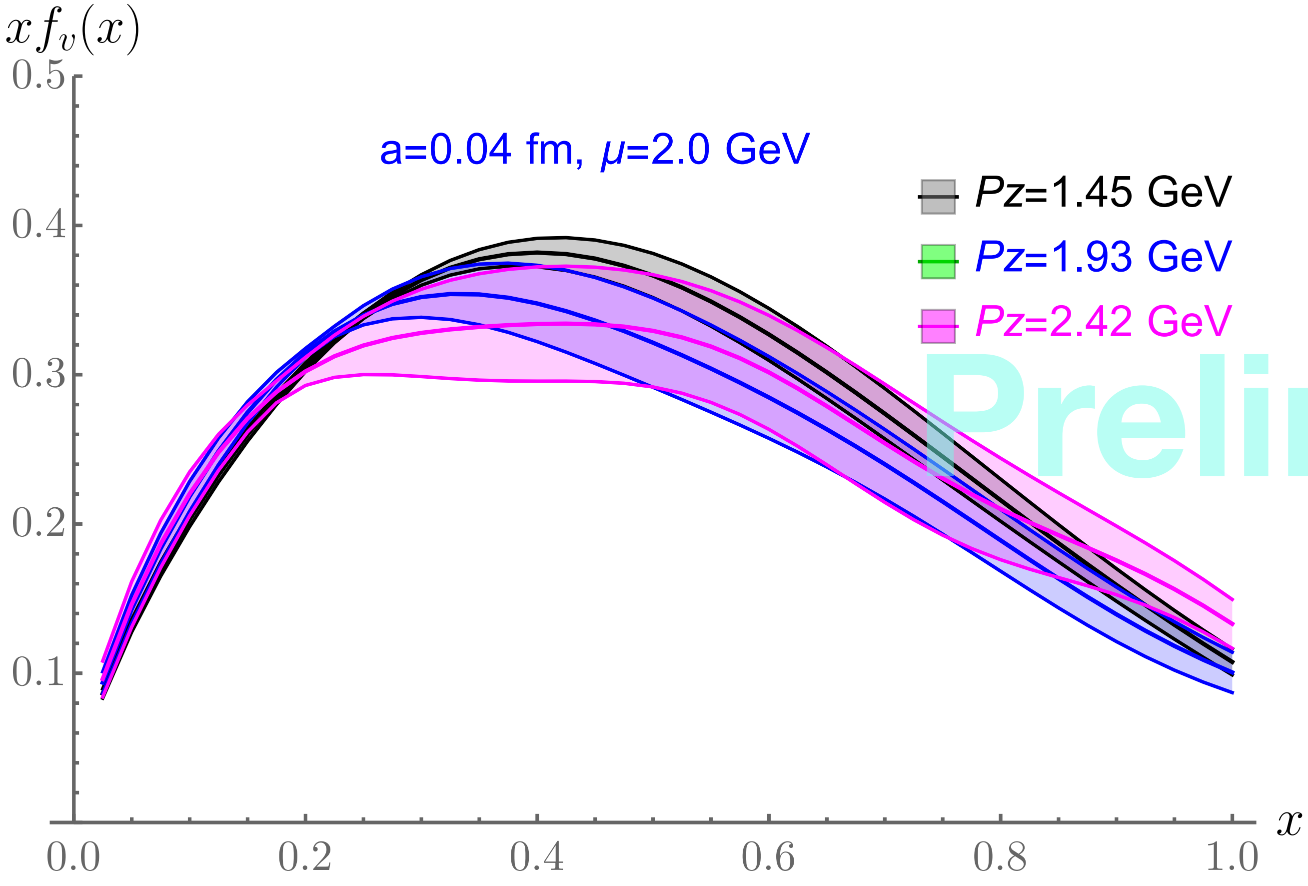

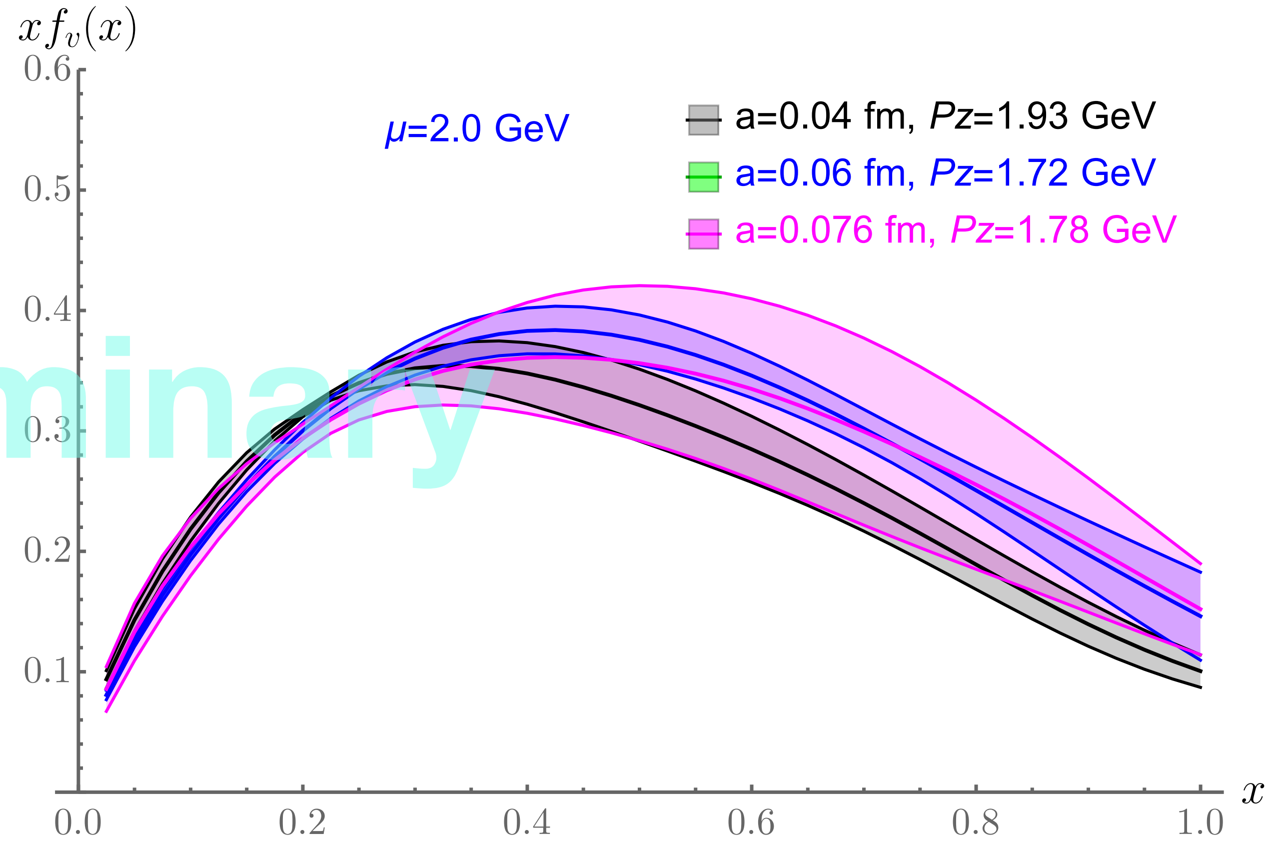

Comparison with previous analysis and phenomenology

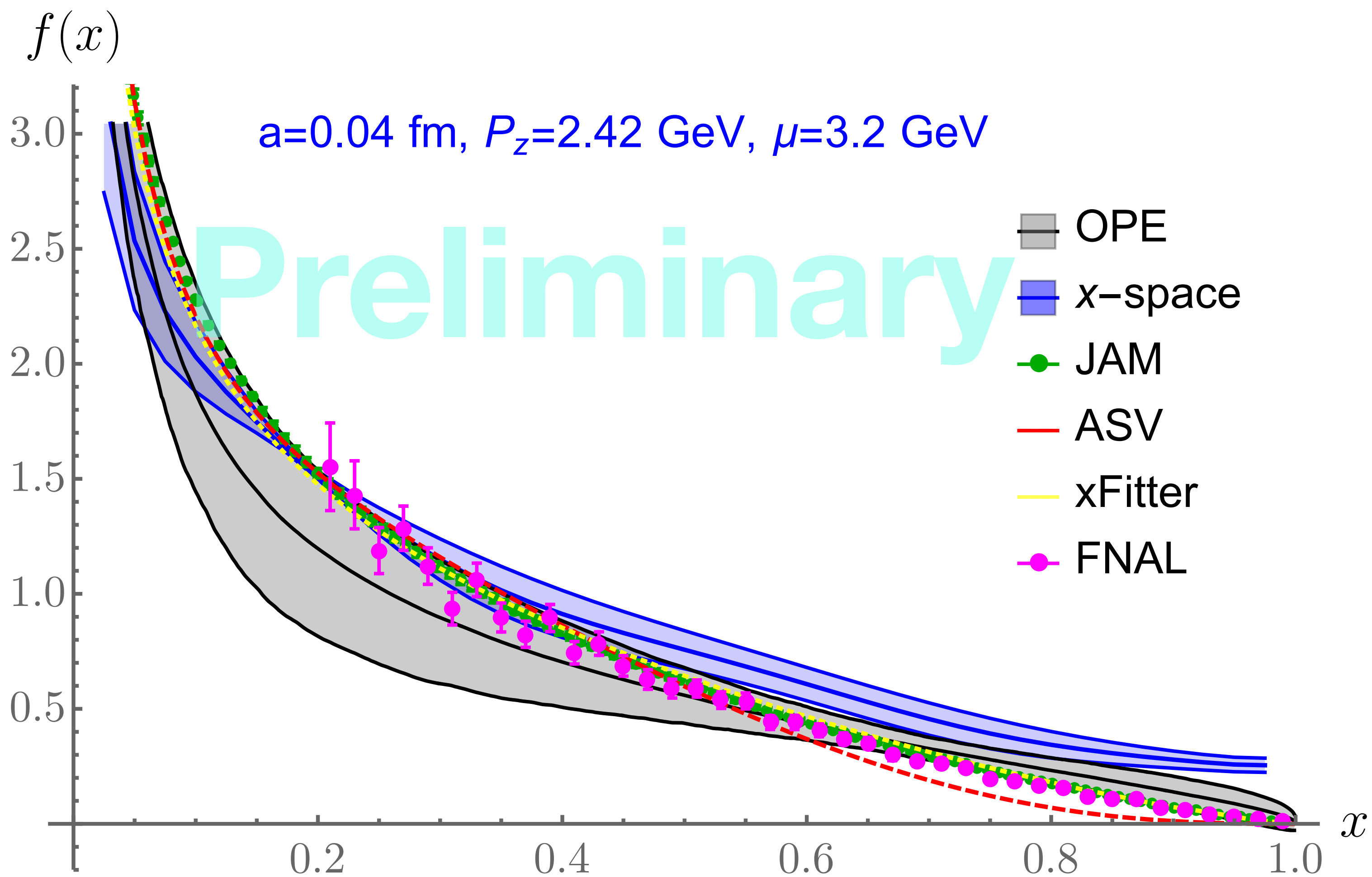

Better agreement with experimental fits for 0.1 < x < 0.45
compared to our previous analysis using OPE in coordinate space.

Outlook: 3D Tomography of the proton

Wigner distributions

(or GTMDs):

$W(x, \vec{k}_T, \vec{b}_T)$

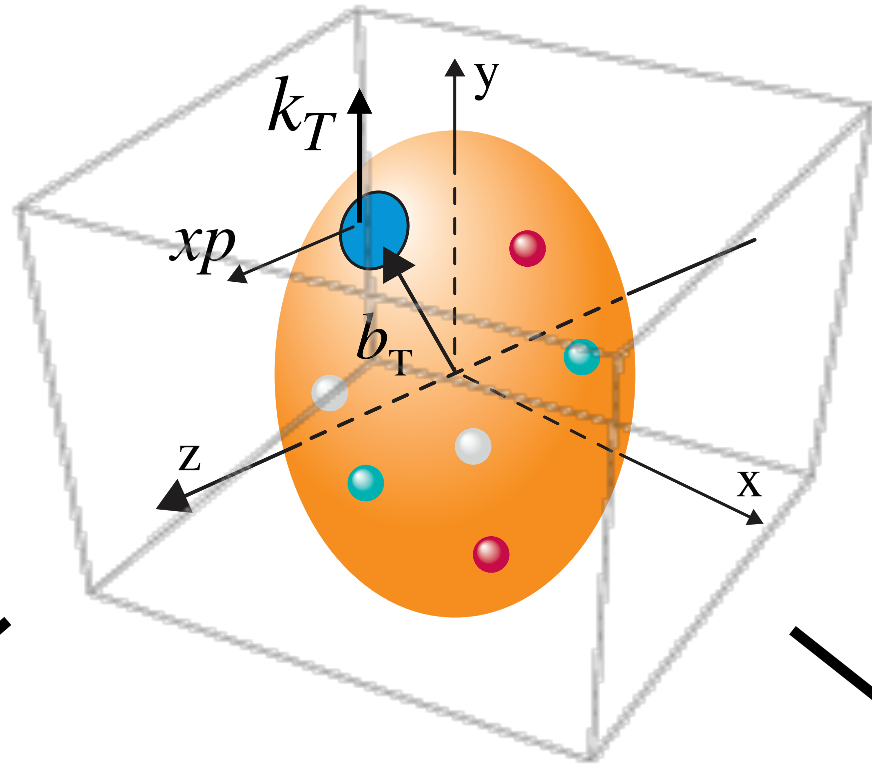

Momentum space:

confined motion

$\int d^2 b_T$

Transverse momentum dependent (TMD) PDFs

$f(x, \vec{k}_T)$

Coordinate space:

spatial distribution

$\int d^2 k_T$

Generalized Parton Distributions (GPDs)

$f(x, \vec{b}_T)$

Lattice calculations of GPDs with LaMET

- Pion valence GPD:

J.W. Chen et al., NPB 952 (2020) 114940.

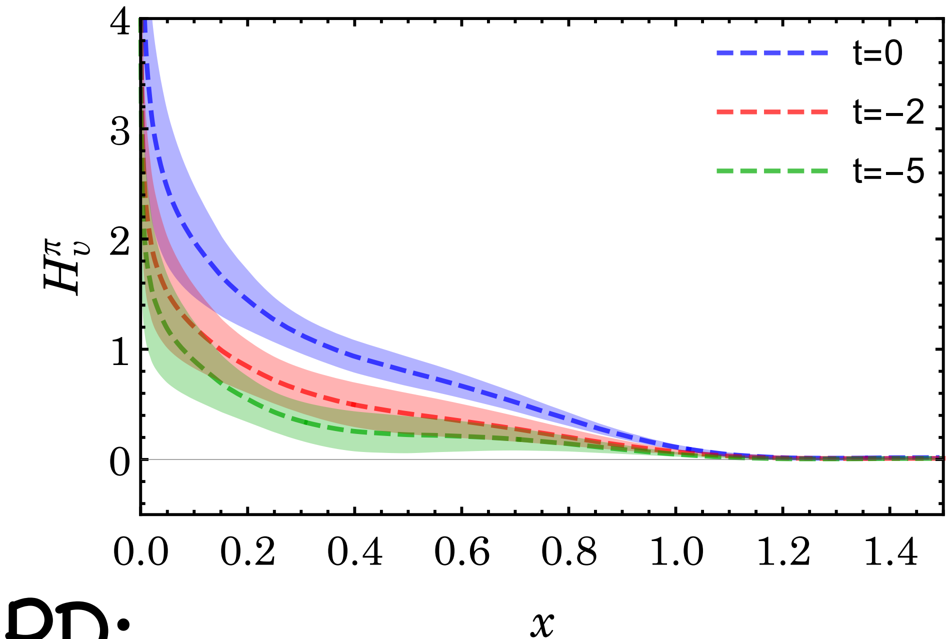

- Proton isovector GPD:

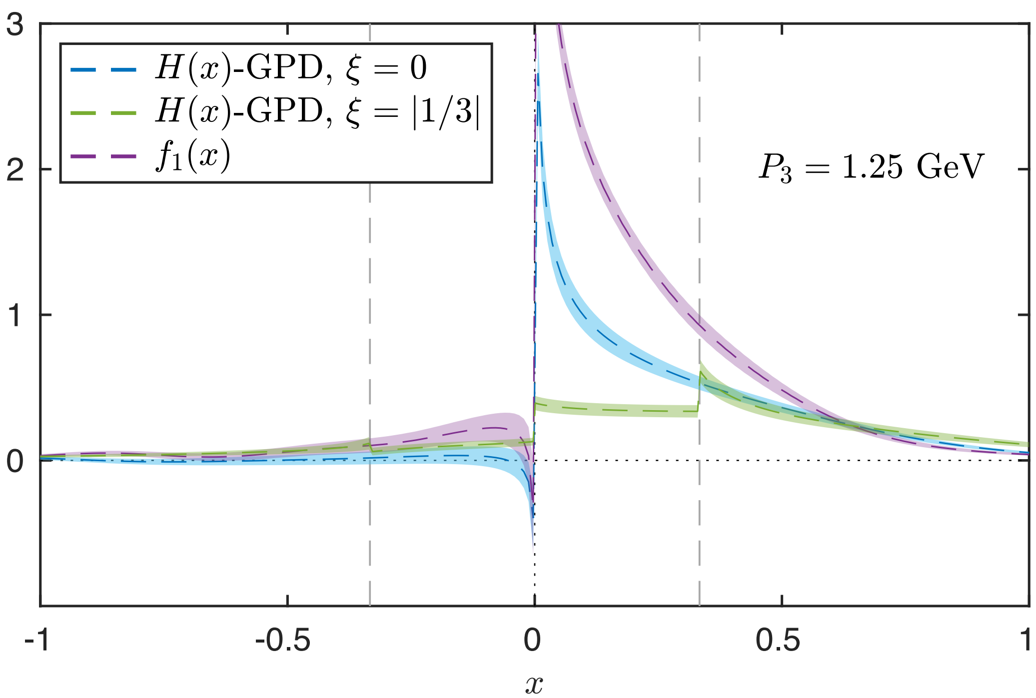

C. Alexandrou et al. (ETM), PRL 125 (2020) 26, 262001. Unpolarized and Helicity cases.

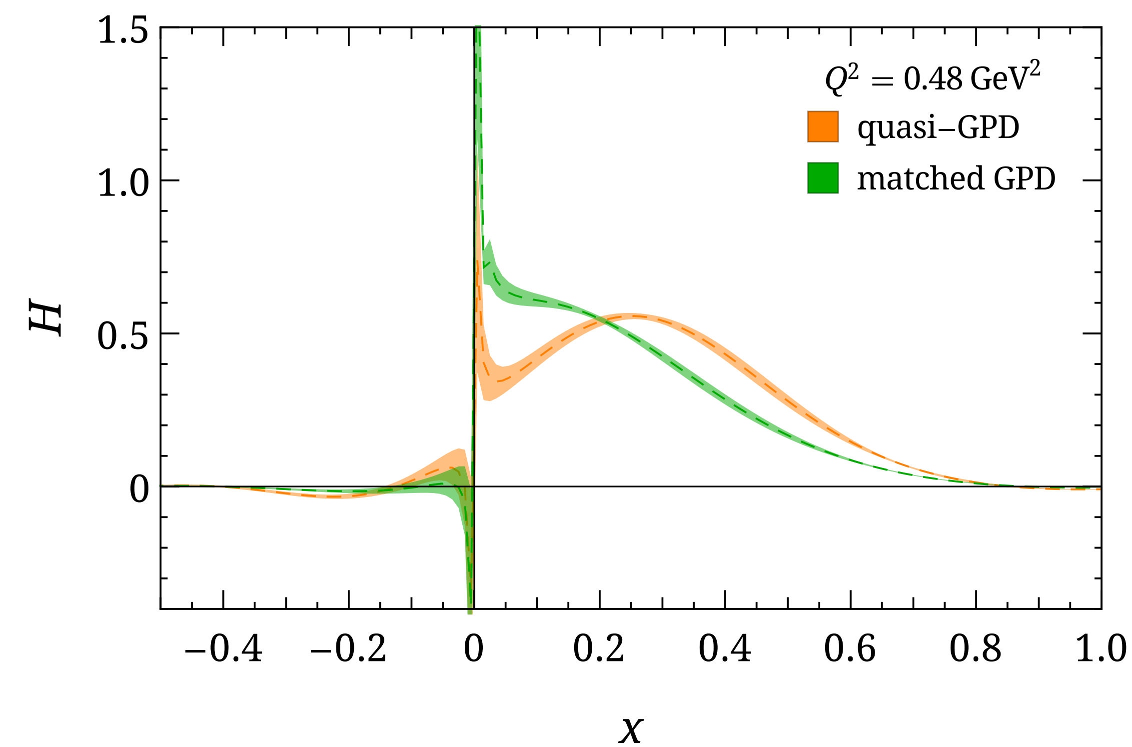

H. W. Lin, 2008.12474.

TMD soft function from lattice QCD

Quasi TMDPDF →

Reduced soft function →

$$\frac{\tilde{f}_{\rm ns}^{\rm TMD}(x, \vec{b}_T, \mu, P^z)}{\sqrt{S_r^q(b_T,\mu)}} = C_{\rm ns}^{\rm TMD}\left(\mu, xP^z\right) \exp\left[\frac{1}{2}\gamma_\zeta^q(\mu, b_T)\ln\frac{(2xP^z)^2}{\zeta}\right] \times f_{\rm ns}^{\rm TMD}(x, \vec{b}_T, \mu, \zeta) + \mathcal{O}\left(\frac{b_T}{L}, \frac{1}{b_T P^z}, \frac{1}{P^z L}\right)$$

(Nonperturbative) Collins-Soper evolution kernel

- Ji, Sun, Xiong and Yuan, PRD91 (2015);
- Ji, Jin, Yuan, Zhang and YZ, PRD99 (2019);
- M. Ebert, I. Stewart, YZ, PRD99 (2019), JHEP09 (2019) 037.
- Ji, Liu and Liu, Nucl.Phys.B 955 (2020), Phys.Lett.B 811 (2020).

First lattice calculation:

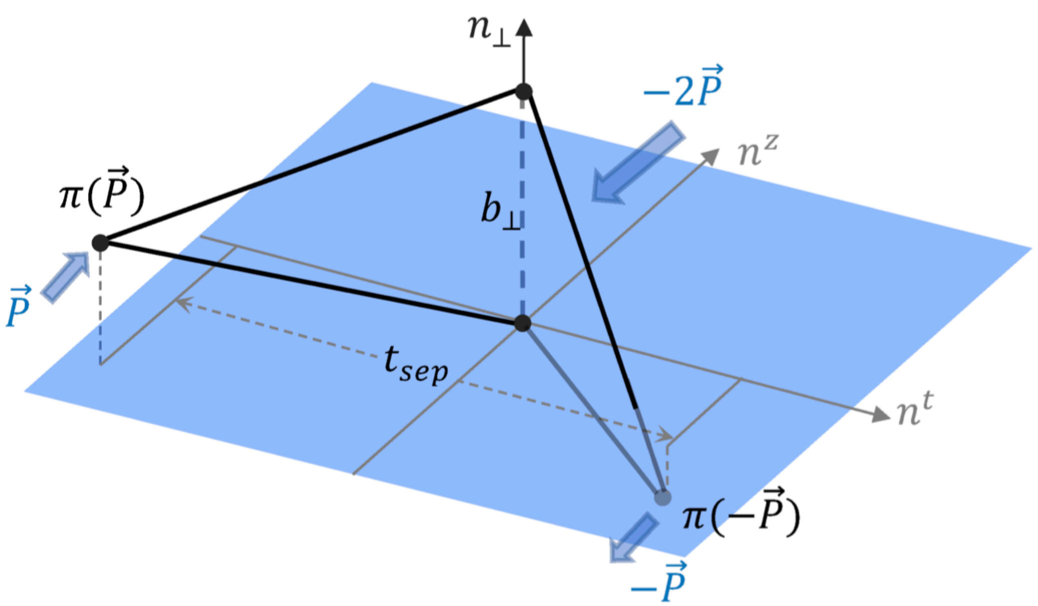

$F(b_T, P^z)$

$S_q^r(b_T, \mu)$

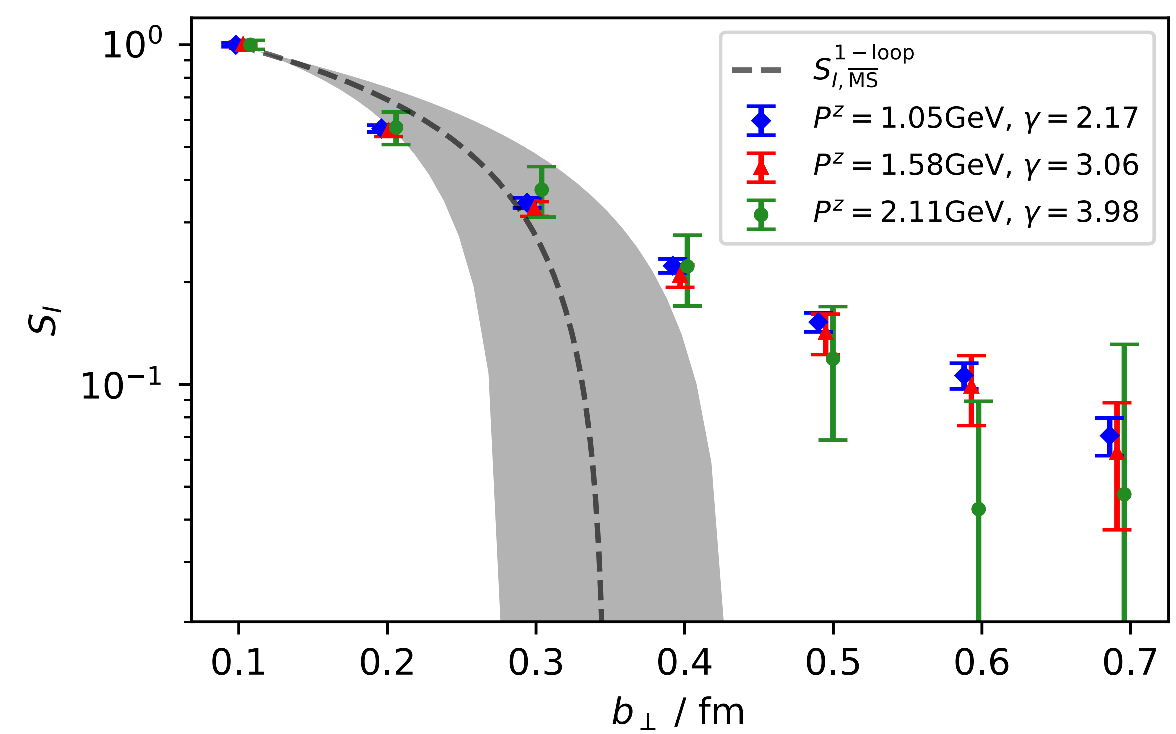

- Ji, Liu and Liu, Nucl.Phys.B 955 (2020), Phys.Lett.B 811 (2020);
- Q.-A. Zhang, et al. (LP Collaboration), Phys.Rev.Lett. 125 (2020).

Collins-Soper kernel from lattice QCD

First exploratory calculation on a quenched lattice ensemble

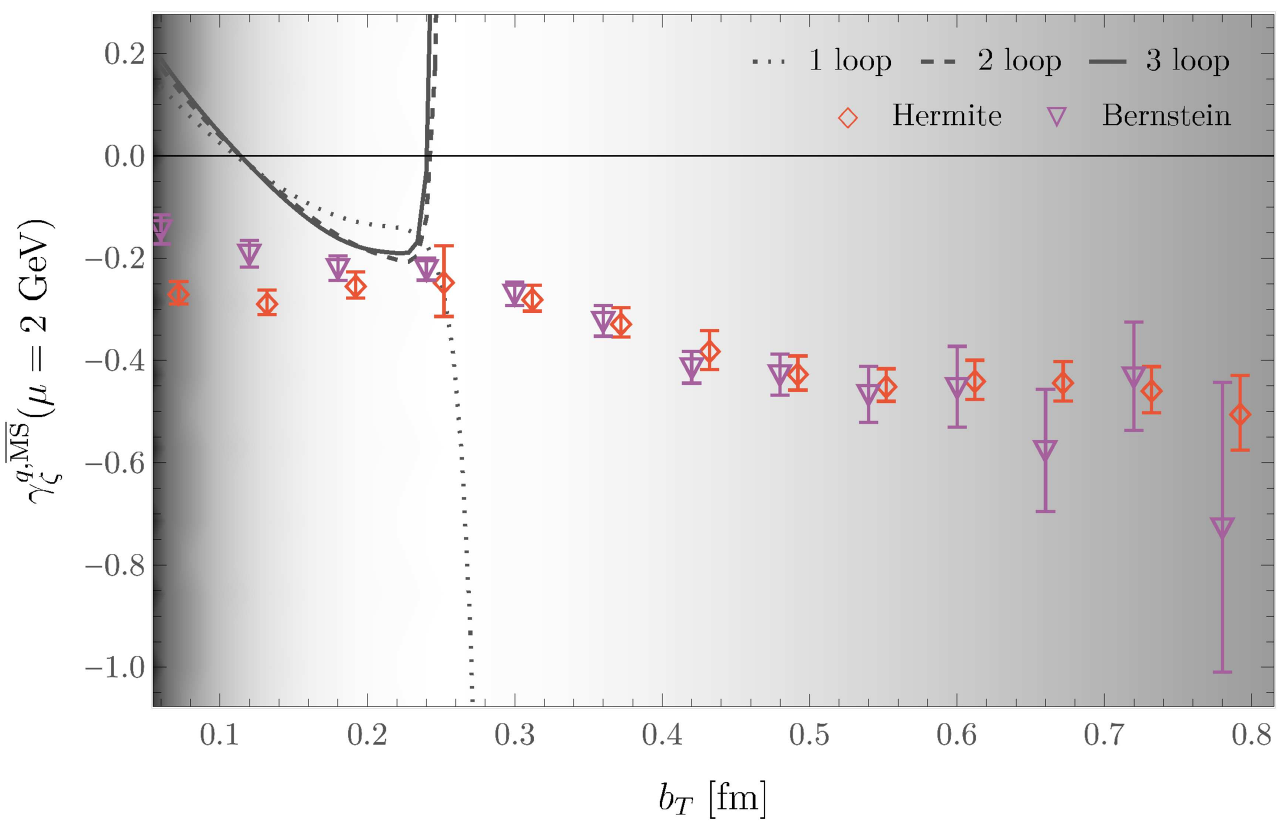

- M. Ebert, I. Stewart, YZ, PRD99 (2019);
- Shanahan, Wagman, YZ, Phys.Rev.D 101 (2020);
- Shanahan, Wagman, YZ, Phys.Rev.D 102 (2020).

Preliminary results with dynamical fermions

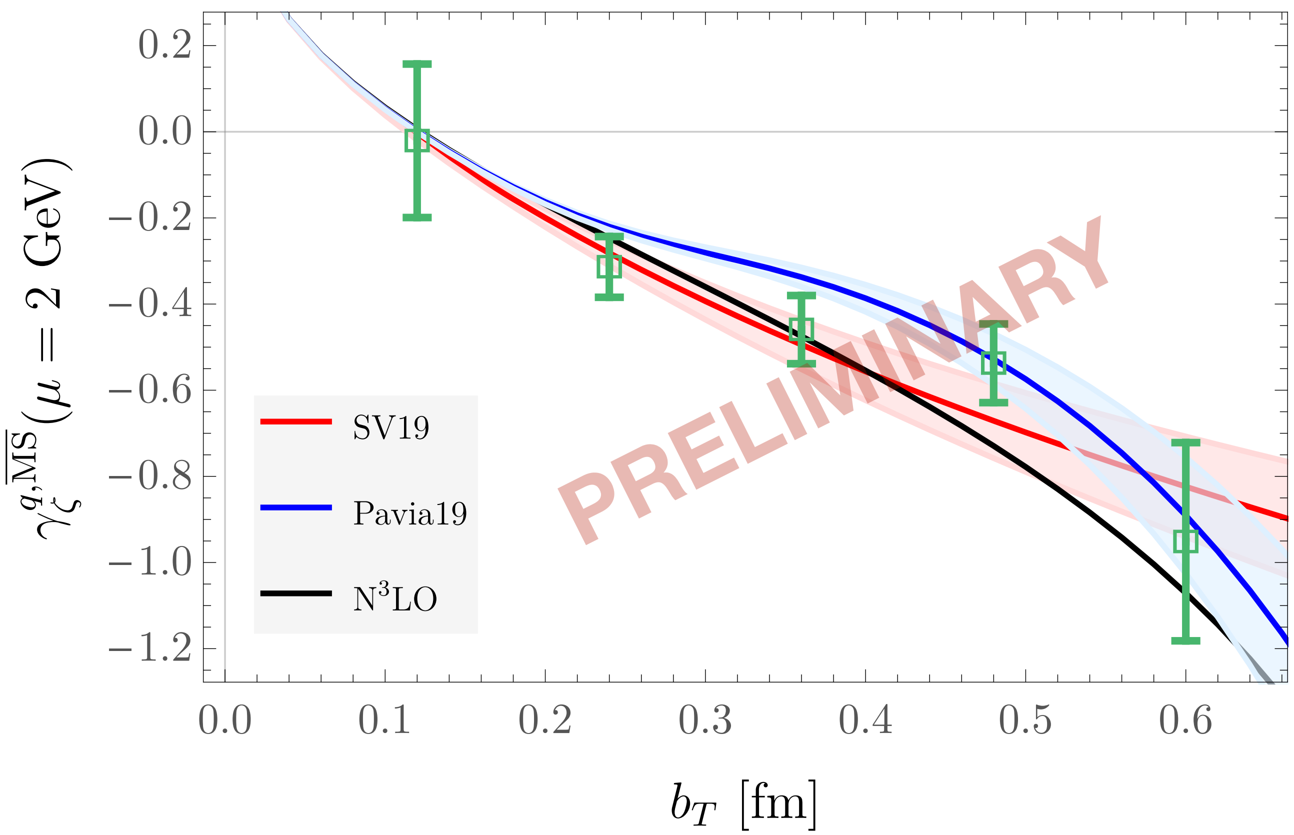

Shanahan, Wagman, YZ, in preparation.

Conclusion

- LaMET allows for model-independent lattice calculation of the x-dependence of the PDFs with controlled systematics;
- The Wilson-line mass renormalization in the hybrid scheme can be well determined from lattice;
- NNLO matching shows good perturbative convergence. We are entering the stage of high-precision calculation of the PDFs;
- LaMET can also be used to calculate GPDs and TMDs, with encouraging progress being made.

Nonperturbative renormalization schemes

$$O_B^\Gamma(z,a) = \bar\psi_0(z)\Gamma W_0[z,0]\psi_0(0) = e^{\delta m|z|}\, Z_{j_1}(a)Z_{j_2}(a)O_R^\Gamma(z)$$

[Ji, Zhang and YZ, 1706.08962; Ishikawa, Ma, Qiu and Yoshida, 1707.03107, Green, Jansen and Steffens, 1707.07152.]

Mass subtraction: $Z_X = e^{\delta m|z|}Z_{j_1}Z_{j_2}$

[Musch et al., 1011.1213;
Ishikawa, Ma, Qiu and Yoshida, 1609.02018;
Chen, Ji and Zhang, 1609.08102;
Green, Jansen and Steffens, 1707.07152.]

- δm: includes linear divergence, can be determined from e.g. static $q\bar q$ potential, etc.;
- Z_j: Renormalization of the "heavy-to-light" current, independent of z;
- Corresponds to the MSbar scheme.

RI/MOM: $Z_X = \langle q\,|\,O^\Gamma(z)\,|\,q\rangle$

[Constantinou and Panagopoulos, 1705.11193;
I. Stewart and YZ, 1709.04933;
C. Alexandrou et al., 1706.00265;
Chen et al., 1706.01295.]

- Perturbative window: $\Lambda^2_{\rm QCD} \ll -q^2 \ll 1/a^2$
- Still introduces nonperturabtive z-dependence as $z \gtrsim \Lambda^{-1}_{\rm QCD}$

Ratio schemes: $Z_X = \langle P_0^z = 0\,|\,O^\Gamma(z)\,|\,P_0^z = 0\rangle$ [A. Radyushkin, 1705.01488; K. Orginos, et al., 1706.05373]

$P_0^z \neq 0$ considered by [X. Gao, et al. (BNL/SBU/THU), 2007.06590].

$Z_X = \langle \Omega\,|\,O^\Gamma(z)\,|\,\Omega\rangle$

[Braun, Vladimirov and Zhang, 1810.00048; Li, Ma and Qiu, 2006.12370.]

- Introduces higher-twist effects as $z \gtrsim \Lambda^{-1}_{\rm QCD}$.

Nonperturbative renormalization schemes

Scheme	Small z	Large z
Mass subtraction	Not the expected $\ln z^2$ behavior due to discretization effects when $z\sim a$, e.g., the function $\ln[(z^2+a^2)/a^2]$	Well defined except for $\mathcal{O}(\Lambda_{\rm QCD})$ ambiguity in the Wilson line mass correction.
RIMOM	$\ln z^2$ dependence cancelled out, therefore the discretization error is cancelled to a large degree	Uncontrolled nonperturbative z-dependence
Ratios		Uncontrolled higher-twist effects

A cancellation of higher-twist effects in the ratio? Cannot be quantified.